cIAP2 was analyzed on cancer and corresponding normal tissues from colorectal cancer patients with curative operations followed by fluorouracil-based adjuvant chemotherapies.

Materials and Methods

Cell lines and reagents. The human colon cancer cell lines (Clone A, COLO205, COLO320, CX-1, DLD-1, HCT-8, HCT-15, HCT116, HT-29, KM12C, LoVo, LS174T, LS180, MIP101, RKO, SW48, SW480, SW620, SW948, SW1116, T84 and WiDr-TC) were either provided from the Cell Resource Center for Biomedical Research, Institute of Development, Aging and Cancer, Tohoku University (Sendai, Japan), or purchased from RIKEN BioResource Center (Tsukuba, Japan) and the American Type Culture Collection (Manassas, VA, USA). The 5-FU-resistant subclone DLD-1/FU was generously provided from Dr M. Fukushima (Taiho Pharmaceutical, Co. Ltd, Tokyo, Japan). The DLD-1/FU cell line was originally derived from the DLD-1 cell line by continuous *in vitro* exposure of DLD-1 cells to increasing concentrations of 5-FU through a number of successive passages, as described earlier.[23] The cells were cultured in either the recommended medium: RPMI1640 (Sigma-Aldrich, St. Louis, MO, USA), L-15 Medium Leibovitz (Sigma-Aldrich), 1 × McCoy 5A (MP Biomedicals, Solon, OH, USA), or D-MEM/F-12 (Invitrogen, Carlsbad, CA, USA), containing 10% heat-inactivated fetal bovine serum (FBS; Sigma-Aldrich, St Louis, MO, USA) and 1% penicillin-streptomycin (Invitrogen). 5-FU was kindly provided by Kyowa Hakko Kogyo (Tokyo, Japan).

Cell proliferation assay and drug cytotoxicity assay. Cells were seeded in 100-mm culture plate at a density of 5×10^4 cells/plate for the cell proliferation assay. On the indicated days, the viable number of cells was determined using a hemocytometer under a light microscope using the trypan blue exclusion method.

Drug-induced cytotoxicity was assessed by the 3-(4,5-dimethylthiazol-2-yl)-5-(3-carboxymethoxyphenyl)-2-(4-sulfenyl)-2H-tetrazolium, inner salt (MTS) assay using the CellTiter 96 Aqueous One Solution Proliferation Assay (Promega, Madison, WI, USA). First, 50 μL of cell suspension was seeded in 96-well plates at a density of 5×10^3 cells/well. All plates were incubated for 24 h at 37°C in a humidified 5% CO_2 atmosphere. Subsequently, 10 dilutions of 5-FU were prepared in growth medium. After incubation, 50 μL of growth medium with diluted 5-FU or growth medium only (as a control) was distributed in 96-well plates. The plates were incubated for 72 h at 37°C. Following incubation, the drugs were removed. Then, fresh medium with MTS was added to each well and the cultures were incubated for 2 h at 37°C. The absorbance of formazan at 490 nm, considered to be directly proportional to the number of living cells in the culture,[24] was measured using a plate reader Multiskan JX (Thermo Fisher Scientific, Yokohama, Japan). The cytotoxic effect of 5-FU was assessed by the 50% inhibitory concentration (IC_{50}: inhibitory drug concentration that results in 50% cell survival) value. With the approximation formula obtained from the straight-line portion of the graph showing the cell survival rate for each dilution of drug, the IC_{50} value was calculated for subsequent analysis.

Total RNA isolation and reverse transcription. Total RNA was extracted from cell lines using the RNeasy Mini Kit (Qiagen, Valencia, CA, USA). The quality and quantity of the extracted total RNA were confirmed by electrophoresis on 1.2% denaturing agarose gels. cDNA was synthesized using a SuperScript III First-Strand Synthesis System for Reverse Transcription – Polymerase Chain Reaction (RT-PCR) Kit (Invitrogen) from 5 μg of total RNA. All the processes were carried out according to the manufacturer's instructions.

cDNA microarray analysis. The CodeLink Uniset Human 20KI Expression Bioarray (GE Healthcare Bio-Sciences, Piscataway, NJ, USA) was used for the cDNA microarray analysis. cRNA synthesis was carried out following the manufacturer's instructions. All of the following reagents were included in the CodeLink Expression Assay Reagent Kit (GE Healthcare Bio-Sciences). First-strand cDNA was generated from 2 μg of total RNA using reverse transcriptase and T7 oligo(dT) primer. Subsequently, second-strand cDNA was produced using *Escherichia coli* DNA polymerase mix and RNase H. The resultant double-stranded cDNA was purified on QIAquick PCR Purification Kit (Qiagen) and cRNA as a probe for microarray was generated by *in vitro* transcription reaction using T7 RNA polymerase and biotin-11-UTP (Perkin Elmer, Boston, MA, USA). cRNA was purified on the RNeasy Mini Kit (Qiagen), quantified by spectrophotometry and 10 μg was then fragmented by heating at 94°C for 20 min in the presence of magnesium ions. The fragmented cRNA was hybridized overnight at 37°C in hybridization buffer to each array in an Innova 4080 Shaking Incubator (New Brunswick Scientific, Edison, NJ, USA) for 18 h. After hybridization, the arrays were washed in 0.75 × TNT buffer (1 × TNT: 0.10 M Tris-HCl [pH 7.6], 0.15 M NaCl, 0.05% Tween-20) at 46°C for 1 h followed by incubation with streptavidin-Cy5 at room temperature for 30 min in the dark. The arrays were then washed in 1 × TNT twice for 5 min each followed by a rinse in 0.05% Tween-20 in water and then dried. Glass slides were scanned using a GenePix 4000 A Scanner (Axon Instruments, Union City, CA, USA). The grids of the image spots were adjusted and their signals were analyzed using the CodeLink System Software (GE Healthcare Bio-Sciences). For each cell line, the experiments were performed either two or three times, independently for all of the steps through cell culture to microarray experiment, to confirm the reproducibility of experiments. To compare the gene expression values from the various experiments, the following array-based normalization was applied. In each array experiment, a set of values was log-transformed and Z-normalized by the mean and the standard deviation (SD) calculated from the 5th to 95th percentiles of all non-marker genes. An unsupervised hierarchical clustering analysis was applied using Cluster 3.0 and Java TreeView programs.[25,26]

RT-PCR. Gene-specific primer sets were designed using the Primer Express Software ver. 2.0 (Applied Biosystems, Foster City, CA, USA). Real-time RT-PCR using cDNA of cell lines was carried out using the Power SYBR Green PCR Master Mix (Applied Biosystems) following the manufacturer's instructions. Triplicate cDNA of each cell line was applied to 96-well reaction plates. Thermal cycling was carried out in the following steps: one cycle of 95°C for 10 min; then 40 cycles of 95°C for 15 s, 60°C for 1 min. *Glyceraldehyde-3-phosphate dehydrogenase (GAPDH)* was used as an endogenous control. The mRNA expression level of *cIAP2* was normalized to that of the *GAPDH* in the corresponding sample.

Western blotting. Human colon cancer cells were harvested with trypsin/EDTA (edetic acid) and phosphated-buffered saline (PBS)-washed cell pellets were treated with EBC lysis buffer (1% NP-40, 40 mM Tris-HCl pH 8.0, 100 mM NaCl). Electrophoresis was performed using 4–20% Tris-Glycine Gels (Invitrogen) and proteins were electro-transferred onto Sequi-Blot PVDF (polyvinylidene difluoride) Membrane (Bio-Rad Laboratories, Hercules, CA, USA). The membranes were probed with the following primary antibodies: rabbit polyclonal anticIAP2 antibody (Santa Cruz Biotechnology, Santa Cruz, CA, USA), or rabbit polyclonal anti-α actin antibody (AbCam, Cambridge, UK) as a control, at 4°C overnight. The membranes were washed and subsequently incubated with horseradish peroxidase-coupled donkey antirabbit antibody (Santa Cruz Biotechnology) for 60 min. All proteins were visualized using SuperSignal West Pico Chemiluminescent Substrate (PIERCE, Rockford, IL, USA).

RNA interference (RNAi). Human colon cancer cells were trypsinized and plated into 6-well plates. After 24 h, the cells were transfected with 50 nM ON-TARGETplus *SMART*pool cIAP2 siRNA (small interfering RNA; Dharmacon, Lafayette, CO, USA) by using DharmaFECT siRNA Transfection Reagent 4 (Dharmacon) according to the manufacturer's instructions. For control experiments, ON-TARGETplus siCONTROL Non-targeting siRNA

doi: 10.1111/j.1349-7006.2009.01112.x

(Dharmacon) was used under the same conditions. Between 48 and 120 h after transfection, gene silencing was examined with real-time RT-PCR and Western blotting.

Caspase 3/7 assay and flow cytometry analysis with the annexin V/propidium iodide (PI) staining. Caspase 3 and 7 activation assays were performed using the Caspase-Glo 3/7 Assay Kit (Promega) according to the manufacturer's instructions. Briefly, the cells were seeded in 96-well plates at a density of 5×10^3 cells/well. After the cells were treated with 5-FU or distilled water (DW), Caspase-Glo 3/7 Reagent (100 μL) was added to each well. The plate was then incubated at room temperature for 1 h and the luminescence of each sample was measured with a Centro LB960 96-well Luminometer (Berthold Technologies, Natick, MA, USA). Because the luminescence of this assay was proportional to the cell number with the preliminary experiments, caspase 3/7 activity was assessed by the luminescence compensated by cell number.

In addition, apoptosis was measured by the Annexin V-FITC Apoptosis Detection Kit I (BD Biosciences, San Jose, CA, USA). Cells were treated with annexin V-fluorescein isothiocyanate (FITC) and PI according to the manufacturer's protocol and were analyzed by multicolor flow cytometry using FACS Calibur with Cell-Quest Software (BD Biosciences).

Immunohistochemistry. Primary colorectal cancer and corresponding normal tissue specimens were obtained from 40 colorectal cancer patients with locoregional lymph node metastasis in stage III according to the TNM (tumor–node–metastasis) classification. All patients had undergone curative operations at Tohoku University Hospital, from 1999 to 2004, and were treated with fluorouracil-based adjuvant chemotherapies (5-FU/leucovorin, doxifluridine or uracil/tegafur). Written informed consent was obtained from all patients. The median age of the patients was 61.0 years (range 30–76). Nineteen patients were female and 21 were male. The median postoperative follow-up time was 70.5 months (range 13.6–110.7).

Formalin-fixed paraffin-embedded tissue sections (3 μm thick) were deparaffinized in xylene and rehydrated in graded alcohol dilutions. Endogenous peroxidase activity was blocked by 3% hydrogen peroxidase for 10 min at room temperature. Antigen retrieval was performed using an autoclave in 0.01 M citrated buffer (pH 6.0) at 121°C for 5 min. For the reduction of non-specific staining, the sections were exposed to 10% rabbit serum for 30 min. They were incubated at 4°C overnight with goat polyclonal anticIAP2 antibody (R & D Systems, Minneapolis, MN, USA) at 1:200 dilution. Secondary antibody reaction was performed using biotinylated rabbit antigoat antibody (Dako, Copenhagen, Denmark) at 1:800 dilution for 30 min at room temperature and peroxidase-conjugated streptavidin (Nichirei Bioscience, Tokyo, Japan) was used according to the manufacturer's instructions. The reacted sections were visualized using 3,3′-diaminobenzidine solution (1 mM 3,3′-diaminobenzidine, 50 mM Tris-HCl [pH 7.6] and 0.006% H_2O_2) and counterstained with hematoxylin for nuclear staining. Immunoreactivity for cIAP2 expression was graded as positive if >10% of cancer or normal epithelial cells were stained and as negative if <10% of cells were stained.

Statistical analysis. Any statistical significance of the mRNA expression level, caspase activity and time to recurrence was determined using either Student's *t*-test or Mann–Whitney *U*-test. The Chi-square test was carried out to test the association between cIAP2 expression and cancer recurrence. The computer program Statcel2 Software (OMS Publishing, Saitama, Japan) and Microsoft Excel 2007 (Microsoft, Redmond, WA, USA) were used for statistical analysis. Values of $P < 0.05$ were considered to be statistically significant.

Results

The growth rates in DLD-1 and DLD-1/FU and cytotoxicity of 5-FU. The growth rates of parental DLD-1 cells and its 5-FU-resistant subclone DLD-1/FU were equivalent (Fig. 1A). However, 5-FU sensitivity of DLD-1/FU was quite different from that of DLD-1 and the IC_{50} of 5-FU in DLD-1/FU was higher than that in DLD-1 by over 100 times: 55.1 ± 10.7 and 0.488 ± 0.013 μg/mL, respectively (Figs 1B and 2B). Among the 21 cell lines other than DLD-1 and DLD-1/FU, the IC_{50} of 5-FU varied from 0.00998 to 9.96 μg/mL. SW620, HCT-8 and SW480 showed high IC_{50} of 5-FU: 9.96, 4.60 and 4.33 μg/mL, respectively; and WiDr-TC, HCT116 and SW48 showed low IC_{50} of 5-FU: 0.00998, 0.0499 and 0.149 μg/mL, respectively (Fig. 2B).

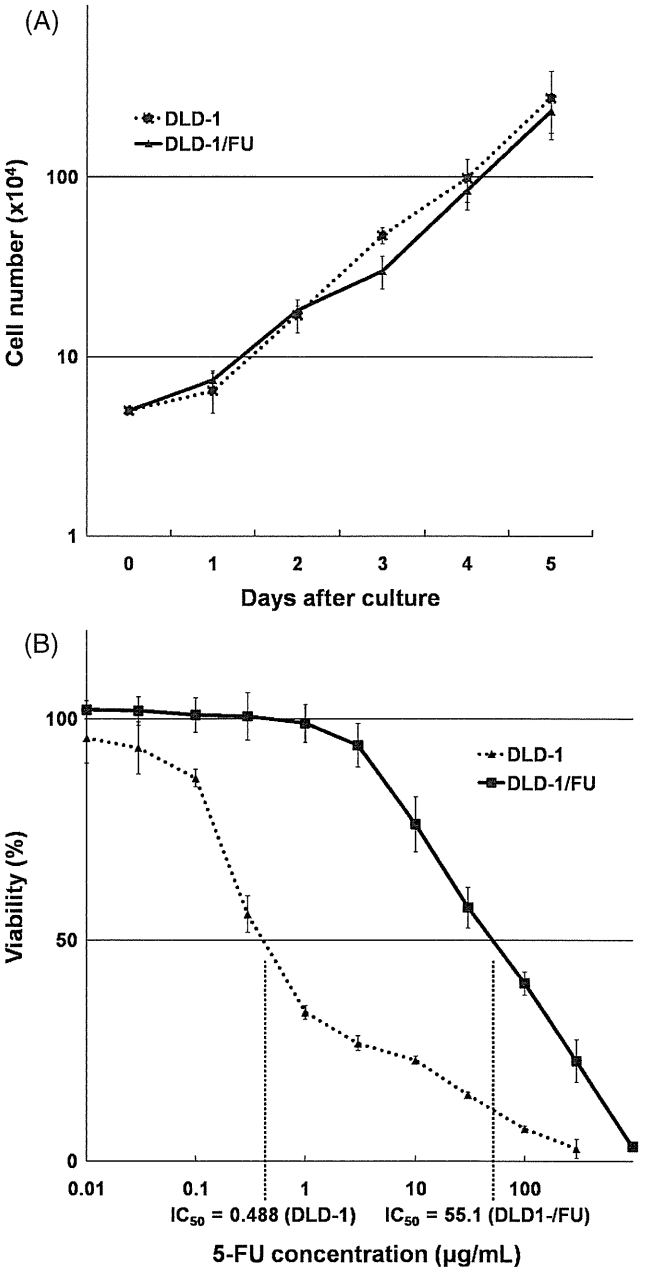

Fig. 1. (A) Proliferation assays of DLD-1 and DLD-1/FU cells. The cell numbers were determined on the indicated days using trypan blue counting. The data represent the means ± SD of triplicate cultures. (B) Cytotoxity of 5-FU and 50% inhibitory concentration in DLD-1 and DLD-1/FU cells. The MTS assay was performed 72 h after treatment with 5-FU. The data represent the means ± SD of three independent experiments.

cDNA microarray analysis and isolation of genes regulating 5-FU resistance. On average 13 472 (67.4%) out of the 19 982 probes in the microarray experiments with the 23 colon cancer cell lines

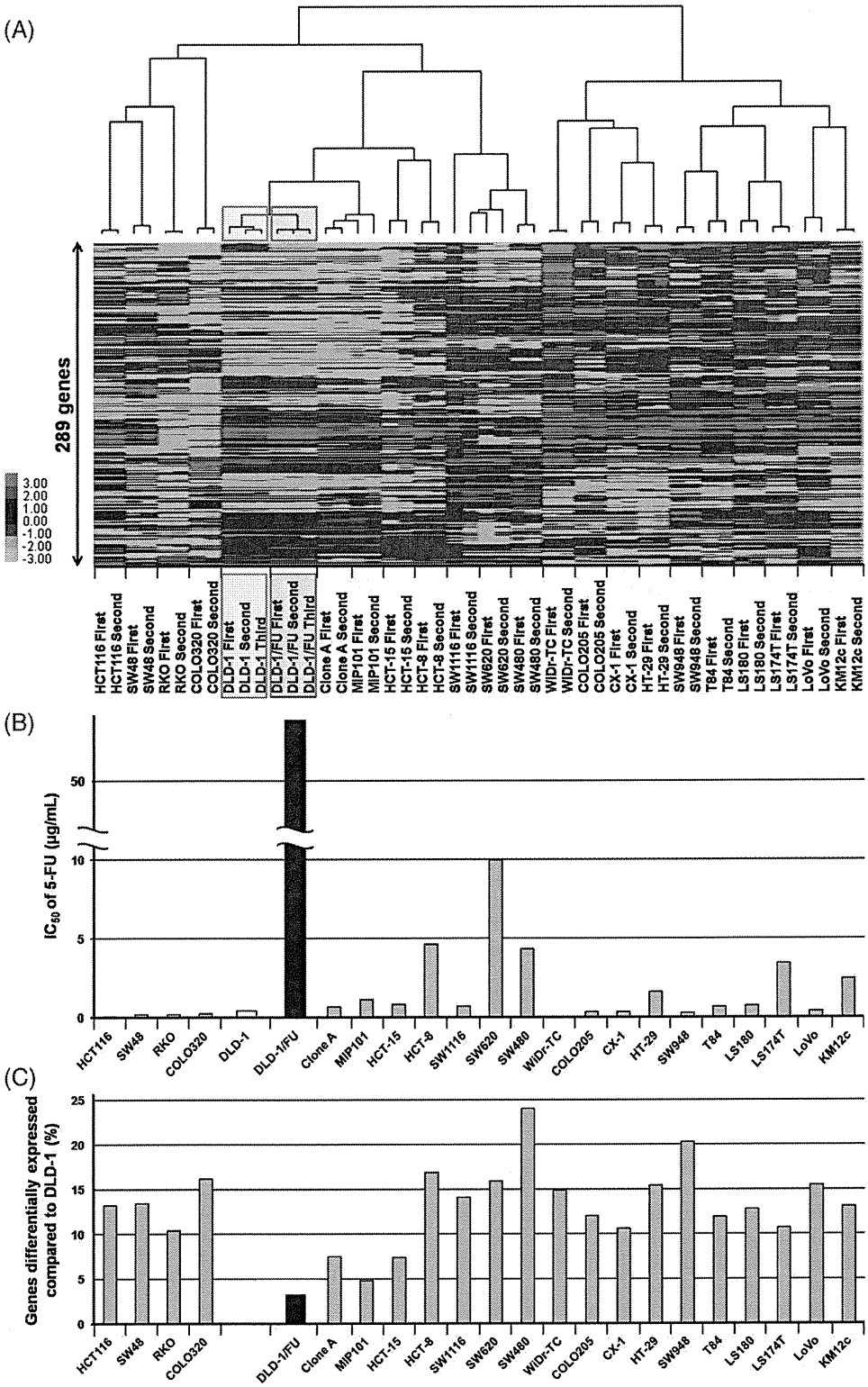

Fig. 2. (A) A dendrogram and its image plot of the hierarchical clustering analysis of 23 colon cancer cell lines including DLD-1 and DLD-1/FU. A cohort of 289 genes out of 13 472 genes, the expression ratios of which varied by SDs of >1.25, were filtered using program Cluster 3.0. (B) The 50% inhibitory concentration of 5-FU in 23 colon cancer cell lines ranged from 0.00998 to 55.1 μg/mL. The data represent the means of two or three independent experiments. (C) Percentages of differentially expressed genes compared to DLD-1. The population of genes with more than a two-fold change in comparison to DLD-1 ranged from 3.3% to 24.0%.

were assessed as 'expressed genes' that gave larger expression values than the 'raw threshold' which was calculated from a set of bacterial marker genes included in the CodeLink microarray as experimental controls.

To evaluate the reproducibility of the microarray experiments and to assess the similarities or differences of gene expression among the colon cancer cells, an unsupervised clustering analysis was performed using 289 genes out of 13 472 genes, the expression

doi: 10.1111/j.1349-7006.2009.01112.x

Table 1. Genes differentially expressed between DLD-1 and DLD-1/FU cells

NCBI Acc. No.	Gene symbol	Gene name	Cytoband	*P*-value	Fold change
Genes highly expressed in DLD1/FU					
NM_006283	TACC1	Transforming, acidic coiled-coil containing protein 1	8p11	1.00E-05	4.41
NM_001903	CTNNA1	Catenin, alpha 1, 102 kDa	5q31	1.46E-06	3.60
NM_017855	ODAM	Odontogenic, ameloblast associated	4q13.3	6.62E-06	3.48
NM_001945	HBEGF	Heparin-binding EGF-like growth factor	5q23	3.54E-06	3.18
NM_015570	AUTS2	Autism susceptibility candidate 2	7q11.22	3.28E-05	2.81
NM_005406	ROCK1	Rho-associated, coiled-coil containing protein kinase 1	18q11.1	9.22E-06	2.80
NM_004815	ARHGAP29	Rho GTPase activationg protein 29	1q22.1	2.03E-05	2.78
NM_012482	ZNF281	Zinc finger protein 281	1q32.1	1.82E-06	2.72
NM_004848	C1orf38	Chromosome 1 open reading frame 38	1p35.3	2.61E-05	2.68
NM_033439	IL33	Interleukin 33	9p24.1	2.45E-05	2.51
NM_001165	BIRC3, cIAP2	Baculoviral IAP repeat-containing 3	11q22	1.99E-05	2.31
NM_024796	FLJ22639	Hypothetical protein FLJ22639	1p36.33	3.94E-05	2.23
NM_012328	DNAJB9	DnaJ homolog, subfamily B, member 9	14q24.2-q24.3	2.51E-05	2.22
NM_006281	STK3	Serin/threonine kinase 3	8q22.2	4.91E-05	2.12
NM_005433	YES1	V-yes-1 Yamaguchi sarcoma viral oncogene homolog 1	18p11.31-p11.21	3.29E-05	2.07
NM_007283	MGLL	Monoglyceride lipase	3q21.3	5.29E-06	2.00
Genes with low expression in DLD1/FU					
NM_000507	FBP1	Fructose-1,6-bisphosphatase 1	9q22.3	9.33E-07	0.16
NM_000873	ICAM2	Intercellular adhesion molecule 2	17q23-q25	8.38E-07	0.18
NM_000295	SERPINA1	Serpin peptidase inhibitor, clade A, member 1	14q32.1	1.99E-05	0.19
NM_000802	FOLR1	Folate receptor 1	11q13.3-q14.1	1.79E-05	0.22
NM_000300	PLA2G2A	Phospholipase A2, group IIA	1p35	4.37E-05	0.23
NM_030763	NSBP1	Nucleosomal binding protein 1	Xq13.3	2.86E-05	0.24
NM_000149	FUT3	Fucosyltransferase 3	19p13.3	1.27E-05	0.34
NM_018725	IL17RB	Interleukin 17 receptor B	3p21.1	5.57E-06	0.34
NM_002889	RARRES2	Retinoic acid receptor responder 2	7q36.1	2.51E-05	0.38
NM_005739	RASGRP1	RAS guanyl releasing protein 1	15q14	2.89E-05	0.45
NM_032355	MON1A	MON1 homolog A	3p21.31	2.87E-05	0.47
NM_000407	GP1BB	Glycoprotein Ib, beta polypeptide	22q11.21	8.30E-06	0.48
NM_003415	ZNF268	Zinc finger protein 268	12q24.33	1.20E-06	0.49
NM_002816	PSMD12	Proteasome 26S subunit, non-ATPase, 12	17q24.2	4.10E-05	0.49
NM_003360	UGT8	UDP glycosyltransferase 8	4q26	3.93E-05	0.50
NM_005116	SCL23A2	Solute carrier family 23, member 2	20p13	9.12E-06	0.50

The expression level of DLD-1/FU was compared to that of DLD-1 with fold change. Listed are genes with *P*-value < 5.0E-05 and fold change >2 or <0.5. NCBI Acc. No., National Center for Biotechnology Information accession number.

ratios of which varied most diversely with SDs of >1.25 (Fig. 2A). In the hierarchical clustering of microarray data of DLD-1 and DLD-1/FU combined with those of another 21 colon cancer cell lines, DLD-1 and DLD-1/FU were most closely clustered. Clone A, which is a subclone isolated from the DLD-1 cell line with an assay using a Boyden chamber,[27] was also clustered together with DLD-1 and DLD-1/FU. The population of genes differentially expressed between DLD-1 and DLD-1/FU cell lines with more than two-fold change was limited to 3.3% (448/13 472 genes; Fig. 2C). On the other hand, in the other 21 colon cancer cell lines, the population of genes differentially expressed with more than a two-fold change in comparison to DLD-1 which was higher than that between DLD-1 and DLD-1/FU, ranging from 4.8% to 24.0% (Fig. 2C). In Clone A and MIP101, which were most closely clustered to DLD-1 and DLD-1/FU with the hierarchical clustering (Fig. 2A), the population of genes differentially expressed with more than a two-fold change in comparison to DLD-1, which was 7.5% and 4.8%, respectively (Fig. 2c). On the other hand, in SW480, SW948, HCT-8, COLO320, SW620, LoVo and HT-29, the population of genes differentially expressed with more than a two-fold change in comparison to DLD-1 which was higher than 15% (Fig. 2C).

To list genes differentially expressed between DLD-1 and DLD-1/FU, two-sample *t*-test was employed. The expression levels of genes in DLD-1/FU were compared to those of DLD-1 with fold change and the genes with *P*-values < 5.0E-05 and with fold change >2 or <0.5 are listed in Table 1. Genes highly expressed in DLD-1/FU which had *P*-values <5.0E-05 and fold change >2 were 16 genes, including *catenin alpha 1 (CTNNA1), heparin-binding EGF-like growth factor (HBEGF)*, and *cIAP2* (also known as *BIRC3*). There were 16 genes with a low expression in DLD-1/FU which had *P*-values <5.0E-05 and a fold change <0.5, including *FBP1*, *ICAM2* and *phospholipase* A2 group IIA (*PLA2G2A*). Subsequently, two categories were specifically focused upon: pyrimidine metabolism-related enzymes and the IAP family (Table 2). In the pyrimidine metabolism-related enzymes, *orotate phosphoribosyl transferase (OPRT)* was down-regulated as had been described in previous reports.[23] In seven genes of IAP family, *cIAP2* was most up-regulated in DLD-1/FU (2.31 times). Using real-time RT-PCR and Western blotting, we reconfirmed the results of cDNA microarray on cIAP2 expression in DLD-1 and DLD-1/FU cells (data not shown).

Down-regulation of cIAP2 by siRNA. The role of cIAP2 on 5-FU resistance in colon cancer cells was further investigated using RNAi. With the data from the microarray and RT-PCR, HCT-8, HT-29, SW948 and WiDr-TC cells showed high expression of the *cIAP2* gene (data not shown). Among the four types of cell lines, HCT-8 and HT-29 were successfully transfected with siRNA and the cIAP2 expression was down-regulated (Fig. 3A). For these reasons, as well as DLD-1/FU cells, HCT-8 and HT-29 cells were chosen for the following experiments using RNAi. At 48 and 120 h after transfection, the down-regulation of cIAP2 was assessed by real-time RT-PCR and 72 h after transfection by Western blotting

Table 2. **Genes differentially expressed between DLD-1 and DLD-1/FU cells involoved in pyrimidine metabolism-related enzymes and IAP family**

NCBI Acc. No.	Gene symbol	Gene name	Cytoband	*P*-value	Fold change
Pyrimidine metabolism-related enzymes					
NM_001071	TYMS, TS	Thymidylate synthetase	18p11.32	7.34E-03	0.80
NM_000373	UMPS, OPRT	Uridine monophosphate synthetase	3q13	3.41E-04	0.57
NM_000110	DPYD, DPD	Dihydropyrimidine dehydrogenase	1p22	–	–
NM_001953	TYMP, TP	Thymidine phosphorylase	22q13.33	–	–
NM_003258	TK1	Thymidine kinase 1, soluble	17q23.2-q25.3	7.51E-03	0.78
NM_004614	TK2	Thymidine kinase 2, mitochondrial	16q22-q23.1	–	–
NM_001033	RRM1	Ribonucleotide reductase M1	11p15.5	N.S.	1.21
NM_001034	RRM2	Ribonucleotide reductase M2	2p25-p24	N.S.	0.83
NM_003364	UPP1	Uridine phosphorylase 1	7p12.3	N.S.	1.08
IAP family					
NM_004536	NAIP, BIRC1	NLR family, apoptosis inhibitory protein	5q13.1	–	–
NM_001166	BIRC2, cIAP1	Baculoviral IAP repeat-containing 2	11q22	N.S.	1.25
NM_001165	BIRC3, cIAP2	Baculoviral IAP repeat-containing 3	11q22	1.99E-05	2.31
NM_001167	XIAP, BIRC4	X-linked inhibitor of apoptosis	Xq25	–	–
NM_001168	BIRC5, SURVIVIN	Baculoviral IAP repeat-containing 5	17q25	N.S.	0.97
NM_016252	BIRC6, APOLLON	Baculoviral IAP repeat-containing 6	2p22-p21	4.82E-02	1.23
NM_022161	BIRC7, LIVIN	Baculoviral IAP repeat-containing 7	20q13.3	N.S.	1.02

The expression level of DLD-1/FU was compared to that of DLD-1 with fold change. NCBI Acc. No., National Center for Biotechnology Information accession number; IAP, apoptosis inhibitory protein; N.S., not significant; –, not reliable for low expressions.

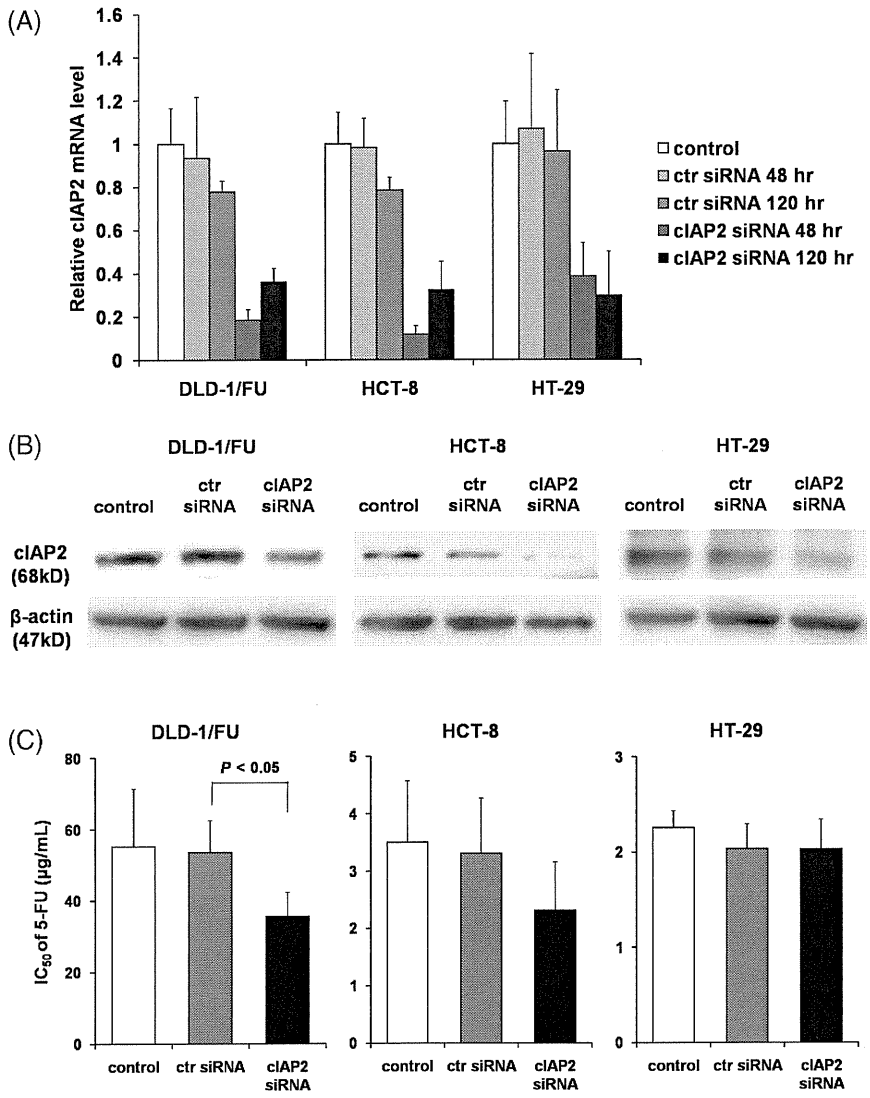

Fig. 3. Down-regulation of cellular inhibitor of apoptosis 2 (cIAP2) by small interfering RNA (siRNA). The messenger RNA (mRNA) and protein levels of cIAP2 were assessed by (A) real-time reverse transcription – polymerase chain reaction or (B) Western blotting in DLD-1/FU, HCT-8 and HT-29 under transfection of cIAP2 siRNA. As controls, untransfected cells (control) and cells transfected with control siRNA (ctr siRNA) were used. mRNA were isolated 48 or 120 h after transfection (Fig. 3a). Cell lysates were collected 72 h after transfection (Fig. 3b). (C) Effect of the down-regulation of cIAP2 on 5-FU sensitivity in human colon cancer cell lines. *In vitro* cytotoxicity assay was performed using MTS assay. At 48 h after transfection with cIAP2 siRNA or control siRNA, 5-FU was added at various concentrations. 72 h after treatment with 5-FU, MTS assay was performed to determine the 50% inhibitory concentration. The results represent the means ± SD of three independent experiments.

doi: 10.1111/j.1349-7006.2009.01112.x

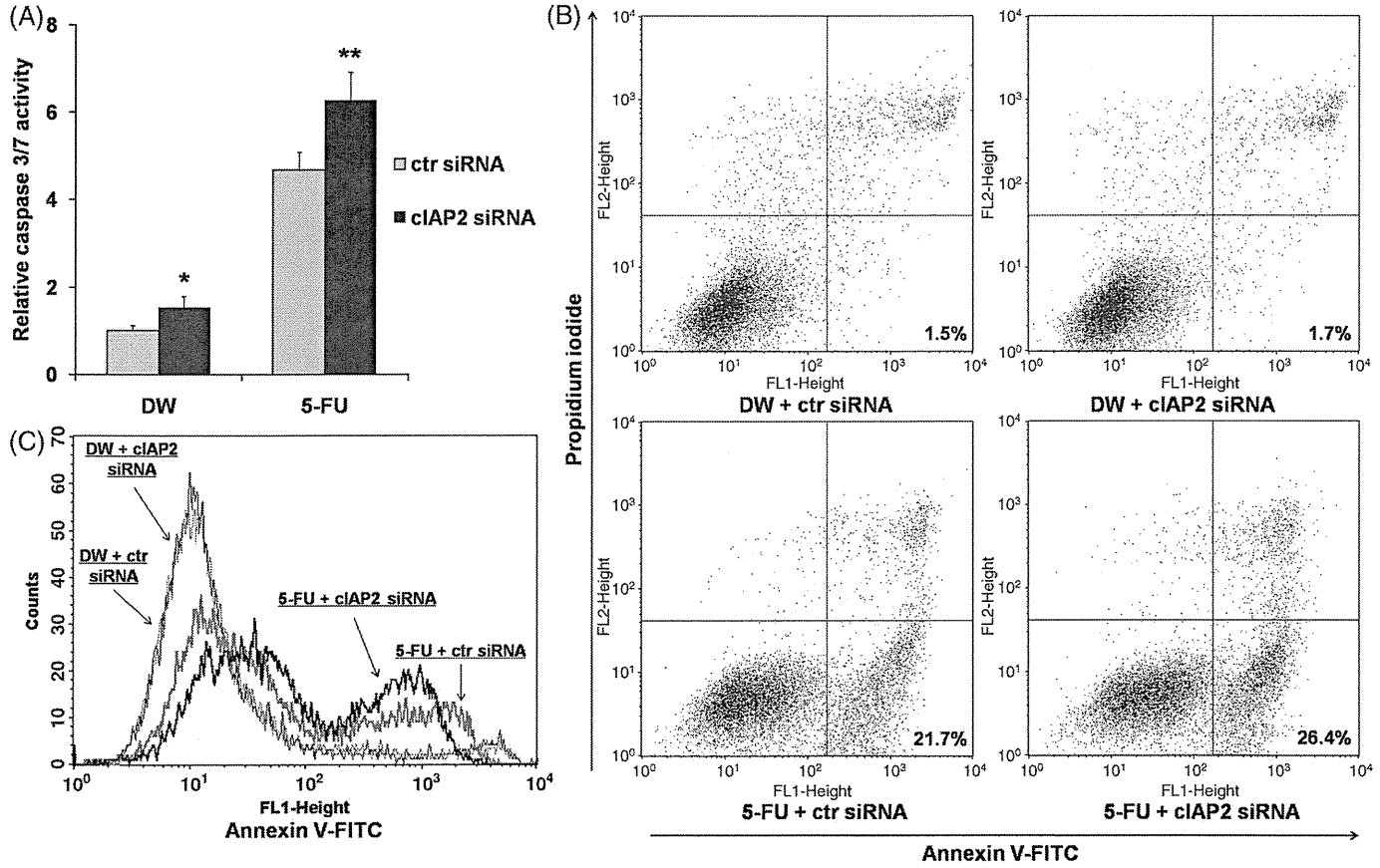

Fig. 4. (A) Down-regulation of cellular inhibitor of apoptosis 2 (cIAP2) induced caspase 3/7 activation. At 48 h after cIAP2 small interfering RNA (siRNA) transfection, cells were exposed to distilled water (DW) or 5-fluorouracil (5-FU) for 48 h and measured for caspase 3/7 activity. As controls, the cells transfected with control siRNA (ctr siRNA) were used. The results represent the ratios to caspase 3/7 activity of untransfected cells with common culture. $*P < 0.05$ *versus* cells treated with ctr siRNA + DW. $**P < 0.05$ *versus* cells treated with each of the other treatments. (B) Incidence of apoptosis in DLD-1/FU revealed by flow cytometric analysis stained with annexin V-fluorescein isothiocyanate (V-FITC) and counterstained with propidium iodide (PI). In cIAP2 siRNA-transfected cells with exposure to 5-FU, the percentage of annexin V-positive/PI-negative cells (early apoptotic cells) shown in the right lower quadrant was high in comparison to the control siRNA-transfected cells. (C) The histogram represents the increase of annexin V-positive fraction in cIAP2 siRNA-transfected cells with exposure to 5-FU. A representative assay out of three independent assays was provided.

(Fig. 3A,B). The expression of cIAP2 was always down-regulated with higher than 50% efficiency, although it could vary depending on the cell types or time points (Fig. 3A,B).

Enhanced 5-FU sensitivity by cIAP2 siRNA. At 48 h after transfection with cIAP2 siRNA or non-targeting siRNA as control siRNA ('ctr siRNA' in Figs 3 and 4), DLD-1/FU, HCT-8 and HT-29 cells were cultured in medium with 10 dilutions of 5-FU and then the IC_{50} was determined by MTS assay. In all of the cell types, treatment with control siRNA did not have a cytotoxic effect on the IC_{50} (Fig. 3C). DLD-1/FU cells transfected with cIAP2 siRNA in the presence of 5-FU showed a significant decrease of the IC_{50} in comparison to those transfected with the control siRNA ($P < 0.05$; Fig. 3C). These results indicate that the down-regulation of cIAP2 in DLD-1/FU cells enhanced the cytotoxicity with 5-FU. The IC_{50} of 5-FU in HCT-8 cells changed in the same manner as in DLD-1/FU ($P = 0.15$); but the IC_{50} of 5-FU in HT-29 cells did not change under the down-regulation of cIAP2 (Fig. 3C).

Activation of caspase 3/7 and induction of apoptosis in DLD-1/FU by cIAP2 siRNA. At 48 h after transfection with cIAP2 siRNA or control siRNA, 5-FU (500 μg/mL) or DW was added to DLD-1/FU cells and the cells were maintained for another 48 h. Then, caspase 3/7 activity was measured and the induction of apoptosis was also analyzed with flow cytometry. As shown in Fig. 4(A), the induction of caspase 3/7 activity was examined in DLD-1/FU cells under the down-regulation of cIAP2 with or without exposure to 5-FU. Without exposure to 5-FU, the caspase 3/7 activity under the down-regulation of cIAP2 was enhanced in comparison to that with control siRNA (with arbitrary units 1.53 *vs.* 0.99, $P = 0.03$; Fig. 4A). After exposure to 5-FU, again the caspase 3/7 activity under the down-regulation of cIAP2 was enhanced in comparison to that with control siRNA (6.26 *vs.* 4.67, $P = 0.02$). Next, as shown in Fig. 4(B), the induction of apoptosis with annexin V and PI staining were examined in DLD-1/FU cells under the down-regulation of cIAP2 with or without exposure to 5-FU. Without exposure to 5-FU, induction of early or late apoptotic cells was not observed under the down-regulation of cIAP2 (subpopulated in the right lower portion or the right upper portion in each graph of Fig. 4B, respectively); but with exposure to 5-FU, the induction of early apoptotic cells under the down-regulation of cIAP2 was seen (26.4%). As shown in Fig. 4(C), with exposure to 5-FU, the fraction of early and late apoptotic cells in DLD-1/FU cells was enhanced under the down-regulation of cIAP2 with two-peaks curves, although it was not observed without exposure to 5-FU.

cIAP2 expression in human colorectal cancer and normal tissues with immunohistochemistry and its effect on the prognosis. Immunohistochemistry for cIAP2 was analyzed on colorectal cancer and corresponding normal tissues from 40 patients who underwent curative operations followed by fluorouracil-based adjuvant chemotherapies. cIAP2 was detected exclusively in the cytoplasm of cancer and normal epithelial cells. Seventy percent of cancer tissues were positive for cIAP2 (28/40 cases; Fig. 5A,D,E), whereas only 20% of the normal tissues were positive (8/40 cases; Fig. 5A,F,G).

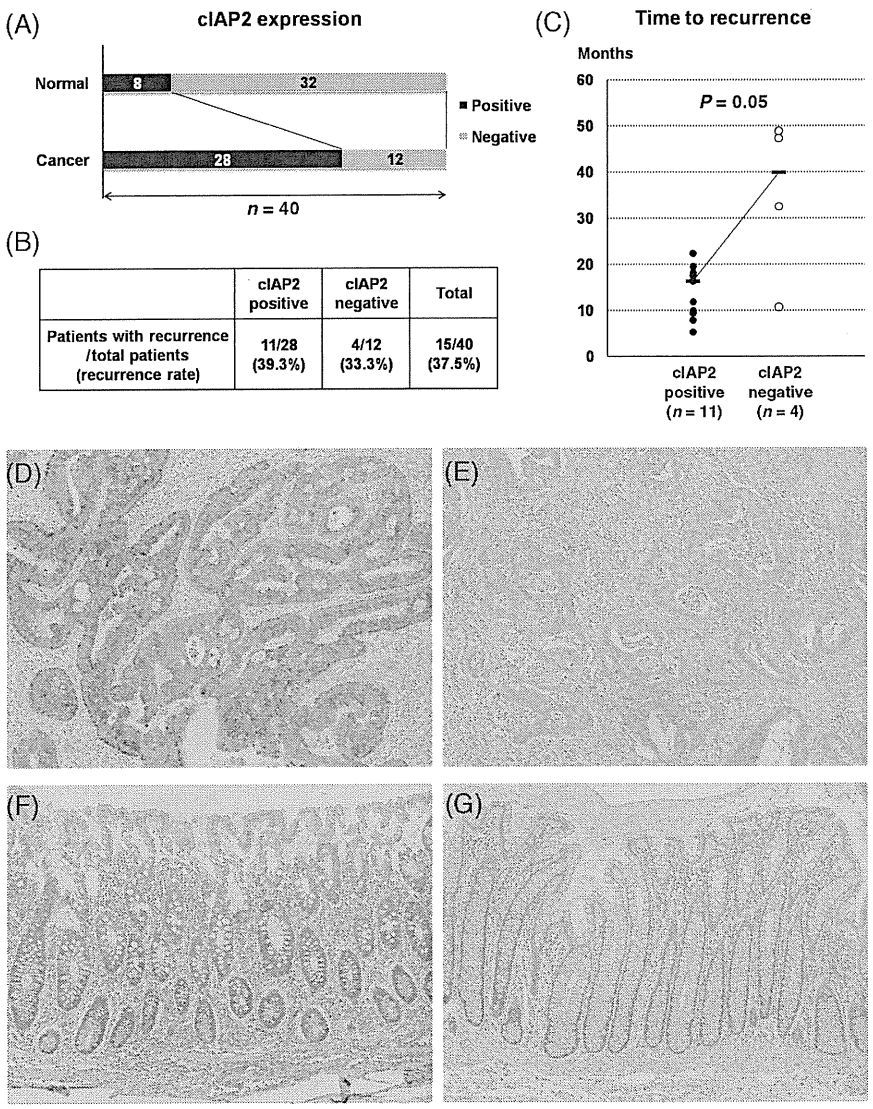

Fig. 5. (A) Cellular inhibitor of apoptosis 2 (cIAP2) expression in human colorectal cancer and the corresponding normal tissues by immunohistochemistry. cIAP2 was more frequently expressed in cancer tissues than in normal tissues. (B) The incidence of cancer recurrence after curative operations in cIAP2-positive and cIAP2-negative patients. (C) The time to recurrence in cIAP2-positive and cIAP2-negative patients. (D–G) Representative image of immunohistochemical staining for cIAP2 in human colorectal cancer and normal tissues (D, cancer tissue/cIAP2-positive; E, cancer tissue/cIAP2-negative; F, normal tissue/cIAP2-positive; G, normal tissue/cIAP2-negative; original magnification: ×100).

Moreover, we analyzed the 40 colorectal cancer patients on the association between cIAP2 expression in the cancer tissues and cancer recurrence. Of the 40 patients, 15 patients (37.5%) experienced cancer recurrence within 5 years after surgery (Fig. 5B). Although we did not find a difference on incidence of cancer recurrence between cIAP2-positive and cIAP2-negative cancer patients (recurrence rate 39.3% *vs.* 33.3%; Fig. 5B), cIAP2-positive cancer patients had a trend to recur earlier after operations than cIAP2-negative cancer patients. Although the number of the cases was limited, we compared the time to recurrence between the two subgroups of the 15 patients: cIAP2-positive patients ($n = 11$) and cIAP2-negative patients ($n = 4$). The time to recurrence in cIAP2-positive patients and cIAP2-negative patients was 16.3 and 39.9 months, respectively ($P = 0.05$; Fig. 5C).

Discussion

Single-drug chemotherapy using 5-FU or its derivatives or combined cytotoxic chemotherapies including 5-FU have been chosen to treat colon cancer. Although anticancer agents and their regimens have been developed, their efficacies have not yet reached a satisfactory level. As Scheithauer *et al.* reported in 1993, the randomized comparison in patients with metastatic colorectal cancers revealed that the median survival time of patients without the use of any form of treatment is in the range of 5 months.[28] According to the Cochrane database,[29] when either fluorouracil alone or fluorouracil combined with leucovorin is administered, the median survival time of patients with metastatic colorectal cancers is extended to 10–12 months. As Salts *et al.*[30] and de Gramont *et al.*[31] reported, the median survival time is prolonged to 14–16 months when either oxaliplatin or irinotecan is added to 5-FU-based chemotherapy. Furthermore, the median survival is prolonged to longer than 20 months when a targeted therapy including bevacizumab or cetuximab is added to the cytotoxic chemotherapies including FOLFOX (folinic acid, FU and oxaliplatin) or FOLFIRI (folinic acid, FU and irinotecan).[4] Currently 5-FU plays a central role in chemotherapies for colorectal cancers and thus it is important to elucidate the mechanisms defining the sensitivity to 5-FU for designing successful chemotherapies. Improvement of 5-FU sensitivity, the selection of agents combined with 5-FU-based chemotherapies and the selection of regimens for individual patients are especially important to achieve better prognosis in advanced colorectal cancer cases.

In the current study, focusing specifically on improving the sensitivity to 5-FU and the selection of types of therapy for each individual patient, to identify novel genes which define the sensitivity or tolerance to 5-FU in colorectal cancers, the expression profiles of the parental DLD-1 cell line was compared to its 5-FU-resistant subclone DLD-1/FU. First, a hierarchical clustering was performed with microarray data of DLD-1 and DLD-1/FU combined with those of 21 other colon cancer cell lines. As shown

doi: 10.1111/j.1349-7006.2009.01112.x

in Fig. 2(A), DLD-1 and DLD-1/FU were most closely clustered and Clone A and MIP101 were also closely clustered. The expression profiles of genes originating from the entire genome will represent the characteristics of cells and this strategy will be good for prediction of the origin of cell types or derived organs; but this strategy will not be good for more precise analyses, including the prediction of sensitivity to some drugs.[32] For such a purpose, it will be necessary to identify a special set of genes. In Fig. 2(A) 289 genes were selected as representatives from the whole set of genes. The expression profiles of DLD-1 and DLD-1/FU cells were quite similar in comparison to the other cell lines, even after the acquisition of 5-FU resistance in DLD-1/FU cells as shown in Fig. 2(B). These results suggest that a change of expression profiles in a limited population of genes contributes to the acquisition of 5-FU resistance in DLD-1/FU cells. Figure 2(C) demonstrates that 3.3% of the genes (448/13 472 genes) were differentially expressed between DLD-1 and DLD-1/FU with more than a two-fold change. In the other 21 colon cancer cell lines, the population of genes differentially expressed with more than a two-fold change in comparison to DLD-1 was higher than that between DLD-1 and DLD-1/FU, ranging from 4.8% to 24.0% (Fig. 2C). This revealed that, as expected, the difference of 5-FU sensitivity was derived from a change of expressions in a limited member of genes. After the acquisition of 5-FU resistance, the secondary or tertiary effects may have affected the changes in expressions in some of the 448 genes; and therefore the number of genes essential for determining the difference in 5-FU sensitivity may be much smaller than 448 genes. Schmidt *et al.* analyzed the change of expression profiles during the establishment of a 5-FU-resistant subclone from the human colon cancer cell line SW620 using a cDNA microarray and the number of genes which showed expression changes in their analysis was limited to 4.8% among the genes they used (330/6888 genes).[33] Their result is consistent with the current findings, both of which suggested that the limited number of genes regulate the sensitivity or resistance to 5-FU in colorectal cancer cells. On the other hand, comparing the hierarchical clustering (Fig. 2A) to the IC_{50} of 5-FU (Fig. 2B) or the population of genes differentially expressed among the 23 colon cancer cell lines (Fig. 2C), it is difficult to identify a correlation. These results show that 5-FU sensitivity is regulated by diverse mechanisms or pathways. As shown in Fig. 3(C), the down-regulation of cIAP2 induced the HCT-8 cell line to become more sensitive to 5-FU, but the 5-FU sensitivity of HT-29 did not change. This may suggest the possibility that the sensitivity to anticancer agents including 5-FU is regulated by a variety of pathways in cancer cells. Harlin *et al.* reported the compensating pathways of IAP functions using a XIAP knock-out mouse.[34] In the current experiments using HT-29, such compensating pathways may therefore have functioned.

In regard to pyrimidine metabolism-related enzymes (Table 2), a comparison between DLD-1 and DLD-1/FU showed that the OPRT gene was down-regulated in DLD-1/FU. The correlation between the expression of OPRT and 5-FU sensitivity was previously described,[35,36] and the current result was consistent with those reports. However, our results on TS and DPD did not support the results reported previously, which may suggest the difficulty of such analyses.

To identify novel genes that regulate 5-FU sensitivity, the expression profiles of DLD-1 and DLD-1/FU were compared and the genes differentially expressed between DLD-1 and DLD-1/FU were listed (Table 1). Among the genes with low expression in DLD-1/FU, the *PLA2G2A* gene, which encodes a group IIA-secreted phospholipase A2, is of particular interest. The expression of *PLA2G2A* has been reported to suppress the progression or metastasis of human gastric cancers.[37] Recently, Ganesan *et al.* also reported that the anti-invasive effect of *PLA2G2A* occurs through its ability to inhibit the *S100A4* gene, which is a metastasis mediator gene in gastric cancer cells.[38] These results may suggest that the expression of the *PLA2G2A* gene may affect the character of cancer cells, including their responses to anticancer drugs such as 5-FU.

In genes highly expressed in DLD-1/FU, some of these genes are of interest from the standpoint of 5-FU resistance. HBEGF, which binds to epidermal growth factor receptor (EGFR)/ErbB1 and ErbB4, is a member of the EGF family. The overexpression of HBEGF has been reported in several types of cancers including colon cancer and pancreatic cancer.[39,40] Suganuma *et al.* identified *HBEGF* as a 5-FU- and cisplatin-resistance-related gene in gastric cancer using cDNA microarray,[41] and Wang *et al.* further investigated the potential role of HBEGF which regulated the chemotherapy-induced EGFR activation,[42] and our results in Table 1 support their findings. Next, *CTNNA1* encodes α-catenin whose interaction with actin-based cytoskeleton is required for the strong state of E-cadherin-based cell adhesion activity.[43] Matsubara *et al.* reported α-catenin expression increases the resistance to apoptosis induced by sphingosine in the colon cancer cell line and α-catenin mediated transduction of signals from the cadherin-catenin complex to regulate the apoptotic cascade.[44] *CTNNA1* is therefore a gene that can possibly regulate drug resistance through the apoptotic pathway.

Among the genes highly expressed in DLD-1/FU, the *cIAP2* gene has drawn a lot of attention and the role of the *cIAP2* gene on 5-FU sensitivity was further analyzed in colon cancer cell lines. In our analysis using RNAi, the down-regulation of cIAP2 changed the phenotype of DLD-1/FU to be more sensitive to 5-FU (Fig. 3C). Lopes *et al.* reported that the expression of cIAP2 protein affected the sensitivity to cisplatin and doxorubicin in pancreatic cancer cell lines.[21] In addition, the expression of IAP family genes, such as survivin and *XIAP*, affect the sensitivity to several types of anticancer drugs in cancers of some organs such as the lung and ovary.[20–22,45–47] However, the association between drug sensitivity and the IAP family in colon cancer has not been reported so far. The current result raises the possibility for novel strategies of cancer chemotherapy in colorectal cancer.

After the down-regulation of cIAP2 by siRNA, the expression level of cIAP2 in DLD-1/FU was almost equivalent to that in its parental cell DLD-1 (Table 1, Fig. 3A); however, the IC_{50} of 5-FU in DLD-1/FU (35.5 μg/mL) was still much higher than that in DLD-1 (0.488 μg/mL). This result suggests that some other genes, such as those listed in Table 1, may also play an important role in regulating 5-FU resistance as well as *cIAP2*.

Although the association between IAPs and drug resistance has been previously discussed, there have been few reports discussing overexpression of IAPs. Although we have not shown the association between cIAP2 overexpression and 5-FU sensitivity in our report, Pratt *et al.* have analyzed survivin overexpression in breast cancer cell line and showed that unexpectedly the increased survivin did not promote paclitaxel resistance.[47] Their results suggest the difficulty in elucidating the association between cIAP2 induction and drug resistance.

With the down-regulation of cIAP2 without 5-FU exposure, the activity of caspase 3/7 was induced, but apoptosis was not induced (Fig. 4). However, with the down-regulation of cIAP2 with 5-FU exposure, apoptosis was efficiently induced (Fig. 4). The results indicate that the activation of the caspase 3/7 pathway is essential for the induction of apoptosis in DLD-1/FU cells; and exposure to 5-FU was required for the induction of the apoptosis in addition to the activation of the caspase 3/7 pathway. As Johnstone *et al.* reported previously,[12] the sensitivity or resistance to anticancer drugs is regulated by interactions between drugs and intracellular targets of the drugs (drug–target interaction); however, depending on the severity of the initial insult, drug-induced damage will also result in catastrophic death or it may initiate a series of secondary effects mediated by various stress signaling pathways leading to cell cycle arrest or cell death.[12] Apoptosis is one of the secondary effects that plays an important role and the caspase cascade is included in the pathways of apoptosis. Recently IAP has been

considered as a novel target of cancer therapy and the efficacy of antisense oligonucleotides or small-molecule IAP antagonists has been reported.[48–50] In colorectal cancer, a target therapy against IAP genes may play an important role in the future.

To further identify the role of cIAP2 and their association with 5-FU resistance in human colorectal cancer, immunohistochemistry for cIAP2 was performed on colorectal cancer and normal tissues from 40 patients who underwent curative operations followed by fluorouracil-based adjuvant chemotherapies. As shown in Fig. 5, cIAP2 was more frequently expressed in cancer tissues than in normal tissues. Moreover cIAP2-positive cancer patients had a trend toward early recurrence after fluorouracil-based adjuvant chemotherapies and this result sufficiently supported our results *in vitro*. It suggested that cIAP2 performed a crucial function and could be a potential therapeutic target in human colorectal cancer.

In conclusion, this study indicated that differences of 5-FU sensitivity could thus be defined by a limited number of genes. Among them, the role of the *cIAP2* gene which regulates 5-FU sensitivity through the apoptotic pathway was elucidated *in vitro*. Moreover, the expression of cIAP2 was frequently observed in human colorectal cancer tissue, and might contribute to cancer recurrence in stage III colorectal cancer patients after fluorouracil-based adjuvant chemotherapy. Therefore, cIAP2 may play a key role and may be a good target for the 5-FU sensitivity in colorectal cancer. On the other hand, in order to develop efficient cancer therapies, it is necessary to consider the diversity of the characteristics of normal cells and hosts, which are regarded as the backgrounds from which cancer cells originate.

Acknowledgments

Grant no. 15659303 and 19659318 for cancer research from Ministry of Education, Culture, Sports, Science and Technology of Japan (K. Miura). We are grateful to Drs S. Ohnuma and K. Masuda (Tohoku University) for helpful discussions and technical advice; Ms. E. Shibuya, H. Fujimura and K. Inabe for technical assistance.

References

1 Giacchetti S, Perpoint B, Zidani R *et al.* Phase III multicenter randomized trial of oxaliplatin added to chronomodulated fluorouracil-leucovorin as first-line treatment of metastatic colorectal cancer. *J Clin Oncol* 2000; **18**: 136–47.
2 Douillard JY, Cunningham D, Roth AD *et al.* Irinotecan combined with fluorouracil compared with fluorouracil alone as first-line treatment for metastatic colorectal cancer: a multicentre randomised trial. *Lancet* 2000; **355**: 1041–7.
3 Cunningham D, Humblet Y, Siena S *et al.* Cetuximab monotherapy and cetuximab plus irinotecan in irinotecan-refractory metastatic colorectal cancer. *N Engl J Med* 2004; **351**: 337–45.
4 Hurwitz H, Fehrenbacher L, Novotny W *et al.* Bevacizumab plus irinotecan, fluorouracil, and leucovorin for metastatic colorectal cancer. *N Engl J Med* 2004; **350**: 2335–42.
5 Hinoda Y, Sasaki S, Ishida T, Imai K. Monoclonal antibodies as effective therapeutic agents for solid tumors. *Cancer Sci* 2004; **95**: 621–5.
6 Wohlhueter RM, McIvor RS, Plagemann PG. Facilitated transport of uracil and 5-fluorouracil, and permeation of orotic acid into cultured mammalian cells. *J Cell Physiol* 1980; **104**: 309–19.
7 Longley DB, Harkin DP, Johnston PG. 5-fluorouracil: mechanisms of action and clinical strategies. *Nat Rev Cancer* 2003; **3**: 330–8.
8 Fojo T, Bates S. Strategies for reversing drug resistance. *Oncogene* 2003; **22**: 7512–23.
9 Zembutsu H, Ohnishi Y, Tsunoda T *et al.* Genome-wide cDNA microarray screening to correlate gene expression profiles with sensitivity of 85 human cancer xenografts to anticancer drugs. *Cancer Res* 2002; **62**: 518–27.
10 Maxwell PJ, Longley DB, Latif T *et al.* Identification of 5-fluorouracil-inducible target genes using cDNA microarray profiling. *Cancer Res* 2003; **63**: 4602–6.
11 Lowe SW, Lin AW. Apoptosis in cancer. *Carcinogenesis* 2000; **21**: 485–95.
12 Johnstone RW, Ruefli AA, Lowe SW. Apoptosis: a link between cancer genetics and chemotherapy. *Cell* 2002; **108**: 153–64.
13 Brown JM, Wouters BG. Apoptosis, p53, and tumor cell sensitivity to anticancer agents. *Cancer Res* 1999; **59**: 1391–9.
14 Chang HY, Yang X. Proteases for cell suicide: functions and regulation of caspases. *Microbiol Mol Biol Rev* 2000; **64**: 821–46.
15 Fuentes-Prior P, Salvesen GS. The protein structures that shape caspase activity, specificity, activation and inhibition. *Biochem J* 2004; **384**: 201–32.
16 Ambrosini G, Adida C, Altieri DC. A novel anti-apoptosis gene, survivin, expressed in cancer and lymphoma. *Nat Med* 1997; **3**: 917–21.
17 Tamm I, Kornblau SM, Segall H *et al.* Expression and prognostic significance of IAP-family genes in human cancers and myeloid leukemias. *Clin Cancer Res* 2000; **6**: 1796–803.
18 Schimmer AD. Inhibitor of apoptosis proteins: translating basic knowledge into clinical practice. *Cancer Res* 2004; **64**: 7183–90.
19 Hunter AM, LaCasse EC, Korneluk RG. The inhibitors of apoptosis (IAPs) as cancer targets. *Apoptosis* 2007; **12**: 1543–68.
20 Yonesaka K, Tamura K, Kurata T *et al.* Small interfering RNA targeting survivin sensitizes lung cancer cell with mutant p53 to adriamycin. *Int J Cancer* 2006; **118**: 812–20.
21 Lopes RB, Gangeswaran R, McNeish IA, Wang Y, Lemoine NR. Expression of the IAP protein family is dysregulated in pancreatic cancer cells and is important for resistance to chemotherapy. *Int J Cancer* 2007; **120**: 2344–52.
22 Bilim V, Yuuki K, Itoi T *et al.* Double inhibition of XIAP and Bcl-2 axis is beneficial for retrieving sensitivity of renal cell cancer to apoptosis. *Br J Cancer* 2008; **98**: 941–9.
23 Murakami Y, Kazuno H, Emura T, Tsujimoto H, Suzuki N, Fukushima M. Different mechanisms of acquired resistance to fluorinated pyrimidines in human colorectal cancer cells. *Int J Oncol* 2000; **17**: 277–83.
24 Cory AH, Owen TC, Barltrop JA, Cory JG. Use of an aqueous soluble tetrazolium/formazan assay for cell growth assays in culture. *Cancer Commun* 1991; **3**: 207–12.
25 de Hoon MJ, Imoto S, Nolan J, Miyano S. Open source clustering software. *Bioinformatics* 2004; **20**: 1453–4.
26 Eisen MB, Spellman PT, Brown PO, Botstein D. Cluster analysis and display of genome-wide expression patterns. *Proc Natl Acad Sci USA* 1998; **95**: 14863–8.
27 Ghoda LY, Savarese TM, Dexter DL, Parks RE Jr, Trackman PC, Abeles RH. Characterization of a defect in the pathway for converting 5′-deoxy-5′-methylthioadenosine to methionine in a subline of a cultured heterogeneous human colon carcinoma. *J Biol Chem* 1984; **259**: 6715–19.
28 Scheithauer W, Rosen H, Kornek GV, Sebesta C, Depisch D. Randomised comparison of combination chemotherapy plus supportive care with supportive care alone in patients with metastatic colorectal cancer. *Br Med J* 1993; **306**: 752–5.
29 Colorectal Meta-analysis Collaboration. Palliative chemotherapy for advanced or metastatic colorectal cancer. *Cochrane Database Syst Rev* 2000: CD001545.
30 Saltz LB, Cox JV, Blanke C *et al.* Irinotecan plus fluorouracil and leucovorin for metastatic colorectal cancer. *Irinotecan Study Group N Engl J Med* 2000; **343**: 905–14.
31 de Gramont A, Figer A, Seymour M *et al.* Leucovorin and fluorouracil with or without oxaliplatin as first-line treatment in advanced colorectal cancer. *J Clin Oncol* 2000; **18**: 2938–47.
32 Ross DT, Scherf U, Eisen MB *et al.* Systematic variation in gene expression patterns in human cancer cell lines. *Nat Genet* 2000; **24**: 227–35.
33 Schmidt WM, Kalipciyan M, Dornstauder E *et al.* Dissecting progressive stages of 5-fluorouracil resistance in vitro using RNA expression profiling. *Int J Cancer* 2004; **112**: 200–12.
34 Harlin H, Reffey SB, Duckett CS, Lindsten T, Thompson CB. Characterization of XIAP-deficient mice. *Mol Cell Biol* 2001; **21**: 3604–8.
35 Inaba M, Mitsuhashi J, Sawada H *et al.* Reduced activity of anabolizing enzymes in 5-fluorouracil-resistant human stomach cancer cells. *Jpn J Cancer Res* 1996; **87**: 212–20.
36 Tokunaga Y, Sasaki H, Saito T. Clinical role of orotate phosphoribosyl transferase and dihydropyrimidine dehydrogenase in colorectal cancer treated with postoperative fluoropyrimidine. *Surgery* 2007; **141**: 346–53.
37 Leung SY, Chen X, Chu KM *et al.* Phospholipase A2 group IIA expression in gastric adenocarcinoma is associated with prolonged survival and less frequent metastasis. *Proc Natl Acad Sci USA* 2002; **99**: 16203–8.
38 Ganesan K, Ivanova T, Wu Y *et al.* Inhibition of gastric cancer invasion and metastasis by PLA2G2A, a novel beta-catenin/TCF target gene. *Cancer Res* 2008; **68**: 4277–86.
39 Ito Y, Higashiyama S, Takeda T, Yamamoto Y, Wakasa KI, Matsuura N. Expression of heparin-binding epidermal growth factor-like growth factor in pancreatic adenocarcinoma. *Int J Pancreatol* 2001; **29**: 47–52.
40 Itoh Y, Joh T, Tanida S *et al.* IL-8 promotes cell proliferation and migration through metalloproteinase-cleavage proHB-EGF in human colon carcinoma cells. *Cytokine* 2005; **29**: 275–82.
41 Suganuma K, Kubota T, Saikawa Y *et al.* Possible chemoresistance-related genes for gastric cancer detected by cDNA microarray. *Cancer Sci* 2003; **94**:

doi: 10.1111/j.1349-7006.2009.01112.x

355–9.
42 Wang F, Liu R, Lee SW, Sloss CM, Couget J, Cusack JC. Heparin-binding EGF-like growth factor is an early response gene to chemotherapy and contributes to chemotherapy resistance. *Oncogene* 2007; **26**: 2006–16.
43 Imamura Y, Itoh M, Maeno Y, Tsukita S, Nagafuchi A. Functional domains of alpha-catenin required for the strong state of cadherin-based cell adhesion. *J Cell Biol* 1999; **144**: 1311–22.
44 Matsubara S, Ozawa M. Expression of alpha-catenin in alpha-catenin-deficient cells increases resistance to sphingosine-induced apoptosis. *J Cell Biol* 2001; **154**: 573–84.
45 Sasaki H, Sheng Y, Kotsuji F, Tsang BK. Down-regulation of X-linked inhibitor of apoptosis protein induces apoptosis in chemoresistant human ovarian cancer cells. *Cancer Res* 2000; **60**: 5659–66.
46 Nomura T, Yamasaki M, Nomura Y, Mimata H. Expression of the inhibitors of apoptosis proteins in cisplatin-resistant prostate cancer cells. *Oncol Rep* 2005; **14**: 993–7.
47 Pratt MA, Niu MY, Renart LI. Regulation of survivin by retinoic acid and its role in paclitaxel-mediated cytotoxicity in MCF-7 breast cancer cells. *Apoptosis* 2006; **11**: 589–605.
48 LaCasse EC, Cherton-Horvat GG, Hewitt KE *et al.* Preclinical characterization of AEG35156/GEM 640, a second-generation antisense oligonucleotide targeting X-linked inhibitor of apoptosis. *Clin Cancer Res* 2006; **12**: 5231–41.
49 Varfolomeev E, Blankenship JW, Wayson SM *et al.* IAP antagonists induce autoubiquitination of c-IAPs, NF-kappaB activation, and TNFalpha-dependent apoptosis. *Cell* 2007; **131**: 669–81.
50 Vince JE, Wong WW, Khan N *et al.* IAP antagonists target cIAP1 to induce TNFalpha-dependent apoptosis. *Cell* 2007; **131**: 682–93.

13

OXIDATIVE STRESS-MEDIATED SIGNALING PATHWAYS BY ENVIRONMENTAL STRESSORS

HIDEKO SONE AND HIROMI AKANUMA
National Institute for Environmental Studies, Tsukuba, Ibaraki, Japan

13.1 INTRODUCTION

Oxidative stress in the form of excess reactive oxygen species (ROS) or reactive nitrogen species (RNS) can affect cells deleteriously or beneficially. Such stress might be generated by intracellular or extracellular sources. Furthermore, oxidative stress can cause various biological effects. Environmental stress is a key contributor to human disease. A number of substances such as metals, particulate materials, smoke, pesticides, and physical agents are environmental stressors [1] that contribute to many diseases. Concerns related to environmental stressor-related diseases such as cancer, chronic lung disease, diabetes mellitus, neurodegenerative diseases, and reproductive disorders have been raised recently. Research efforts elucidating the modes by which environmental stressors influence the development and progression of diseases or exploring preventive approaches are expected to engender further improvements in our knowledge. Understanding environmental stressor-induced influences at the molecular level will also provide a wealth of information related to the exploration of biomarkers for environmental stressor-related diseases [2–4].

The mechanisms of redox adaptation in living bodies and cells might involve multiple influences on an active redox-sensitive signaling pathway, such as ROS metabolism and antioxidant defenses, p53 pathway signaling, nitric oxide (NO) signaling pathway, hypoxia signaling, transforming growth factor (TGF)-β-bone morphogenetic protein (BMP) signaling, tumor necrosis factor (TNF) ligand-receptor signaling, and mitochondrial function (Table 13.1). For example, transcription factors such as nuclear factor-κB (NF-κB), nuclear factor erythroid 2-related factor 2 (Nrf2), c-Jun, and hypoxia-inducible factor-1 (HIF-1) engender increased expression of antioxidant molecules such as superoxide dismutase (SOD), catalase, thioredoxin, and the GSH antioxidant system. Metal ions such as arsenic (III/V) or copper (II) directly influence expression levels of those transcription factors and induce various oxidative stress events including thiol molecule perturbation, generation of oxidative DNA adducts, and induction of oxidative molecular biomarkers [5–8]. Nonmetal chemicals such as retinoic acids and 2,3,7,8-tetrachlorodibenzo-*p*-dioxin (TCDD) are also known to influence the expression of oxidative stress-related genes and proteins during carcinogenesis and during embryonic development [9–12]. In relation to cancer, a growing tumor might also produce intracellular and extracellular oxidative stress, which can modify its malignant features. Endogenous sources of tumor ROS or RNS include impaired intracellular genomes or proteomes, metabolism pathways, and xenobiotic metabolism. Consequently, the study of transcriptional regulation of gene expression in the research field of oxidative stress has been useful for identifying new transregulatory factors or new biomarkers induced by exposure to environmental stressors.

Microarray technology has been used in environmental toxicology and biology studies and has led to the establishment of gene expression signatures profiling

Oxidative Stress in Vertebrates and Invertebrates: Molecular Aspects of Cell Signaling, First Edition.
Edited by Tahira Farooqui and Akhlaq A. Farooqui.

TABLE 13.1 Summary of oxidative stress-mediated signaling pathways

Categorical pathways	Canonical Pathway (orthology)
Reactive Oxygen Species (ROS) Metabolism and Antioxidant Defenses	Glutathione Peroxidases (GPx)
	Peroxiredoxins (TPx)
	Superoxide Dismutases (SOD)
	Genes Involved in Superoxide Metabolism
	Genes Involved in ROS Metabolism
	Other Peroxidases and Antioxidant-Related Genes
p53 Signaling (including DNA damage)	Apoptosis-Related Genes
	Cell Cycle Arrest and Checkpoint
	Regulation of the Cell Cycle
	Regulation of Cell Proliferation, Cell Growth, and Differentiation
	Damaged DNA Binding
	Mismatch, Base-Excision and Double-Strand Break Repair
Nitric Oxide (NO) Signaling Pathway	Genes with NO Synthase and Regulators of NO Biosynthesis
	Genes regulated by NO and NO Signaling Pathway
	Genes Involved in Superoxide Release
	Antiapoptosis Genes
	Genes with Antioxidant and Superoxide Dismutase Activity
	Genes with Glutathione Peroxidase, Oxidoreductase, or Peroxidase Activity
	Transcription Regulators
Hypoxia Signaling	Response to Hypoxia and Signal Transduction, Oxidative Stress
	Genes Related to Stress and Immune Response
	Hemoglobin Complex-Associated Genes
	Peroxidase, Oxidoreductase-Related Genes
	Transcription Factors and Regulators and Protein Binding
	Antiapoptosis Induction of Apoptosis and Caspase Activity
	Protein Biosynthesis, Phosphorylation, and Metabolism
	Cytoskeleton and Other Extracellular Molecules
	Cell Cycle, Cell Proliferation, and Growth Factors
	Carbohydrate, Lipid, One-Carbon Compound Metabolism
	RNA Metabolism
	Cardiac Excitation-Contraction (E-C) Coupling
TGF-β-BMP Signaling	TGF-β superfamily, bmp (bone morphogenetic protein) family members, gdf (growth differentiation factor), activin, and activin receptors
	Smad family members, TGF-β/activin-responsive genes, bmp-responsive genes, molecules regulating signaling of the TGF-β superfamily, adhesion molecules, extracellular matrix structural constituents, other extracellular molecules, transcription factors and regulators
Tumor Necrosis Factor (TNF) Ligand-Receptor Signaling	Caspase activation, caspase inhibition, anti-apoptosis genes, induction of apoptosis, other apoptosis-related genes, jnk signaling pathway, nfκb signaling pathway, tnf superfamily members, tnfr1 and tnfr2 signaling pathway, inflammatory response, transcription regulators
Mitochondria	Mitochondrial processing, mitochondrial transportation Fatty acid biosynthesis

the toxicity of environmental stressors [13, 14]. Statistical methods used for DNA microarray studies are mostly multivariate approaches. Although basic methods treat genes as traits, which is consistent with the rules of experimental design, several approaches have been developed using expression ratio data sets. Such approaches regard the genes as cases and the array plates as variables. Most well-known methods based on singular value decomposition have used principal component analysis [15, 16]. In alternative approaches, our previous reports have described that a Bayesian network technique, which is a probabilistic graphical model that represents a set of variable identities, is applicable to investigation of the gene expression interaction networks and the detection of differences arising in them from exposure to different doses of chemicals [17, 18]. Bayesian network techniques can provide predictive information related to the relations between agents and gene expression signatures in the life science fields [19–21].

This chapter addresses various environmental stressor-induced toxicities in experimental animals such as

rats and humans to elucidate the molecular mechanisms underlying toxicity-induced oxidative stress.

13.2 OXIDATIVE STRESS-MEDIATED SIGNALING PATHWAYS

Cells respond and adapt to environmental signals such as stressors [22–24] through multiple mechanisms that involve communication pathways and signal transduction processes. The impact of oxidative stress on various diseases and aging has been reviewed comprehensively. In particular, free radical-induced oxidative stress plays an important role in cancer development, metabolism-related diseases like diabetes and hypertension, and neurodegenerative disorders [4, 25–36]. Our survey of microarray databases and many other published references has revealed the categorical pathways induced by oxidative stress presented in Table 13.2.

ROS metabolism and antioxidant defenses center upon ROS, which are necessary for biological functions and which regulate many signal transduction pathways by directly reacting with and modifying the structure of proteins, transcription factors, and genes to modulate their functions. Actually, ROS induce expression levels of genes associated with signaling cell growth and differentiation, regulating the activity of enzymes (such as ribonucleotide reductase and peroxidase). Control of ROS levels is achieved by balancing ROS generation with their elimination through ROS-scavenging systems such as superoxide dismutases (SOD1, SOD2, and SOD3), glutathione peroxidase, peroxiredoxins, glutaredoxin, and thioredoxin catalase. The ROS can modulate the activities and expression of many transcription factors and signaling proteins that are involved in stress response and cell survival through multiple mechanisms. Therefore, this category includes glutathione peroxidases (GPx), peroxiredoxins (TPx), superoxide dismutases (SOD), genes involved in superoxide metabolism such as arachidonate 12-lipoxygenase (ALOX12), and copper chaperone for superoxide dismutase (CCS). In fact, p53 signaling plays a central role in coordinating the cellular responses to a broad range of cellular stress factors; p53 functions as a node for organizing whether the cell responds to various types and levels of stress with apoptosis, cell cycle arrest, senescence, DNA repair, cell metabolism, or autophagy. Moreover, p53 controls transactivation of target genes, which is an essential feature of stress response pathways [37–39]. In other words, p53 activation leads to a complicated network of responses to the various stress signals encountered by cells [40–44]. The mitochondrial respiratory chain produces NO, which can generate other RNS when cells are under hypoxic conditions. Although excess ROS and RNS can engender oxidative and nitrosative stress, moderate to low levels of both function in cellular signaling pathways. Especially important are the roles of these mitochondrion-generated free radicals in hypoxic signaling pathways, which have important implications for cancer, inflammation, and various other diseases [25, 45]. Hypoxic signaling events include vasodilation, modulation of mitochondrial respiration, and cytoprotection following ischemic insult. These phenomena are attributed to the reduction of nitrite anions to NO if local oxygen levels in tissues decrease [46], which activates the expression of genes through oxygen-sensitive transcription factors including HIF and NF-κB. Hypoxia-dependent gene expression can have important physiological or pathophysiological consequences for an organism, depending upon the cause of the hypoxic insult [47]. These NO signaling and hypoxia signaling pathways are linked to the p53 pathway [48], because recent studies have shown that HIF2α inhibition promotes p53-mediated responses by disrupting cellular redox homeostasis, thereby permitting ROS accumulation and DNA damage [49]. Reportedly, hypoxia activates the tumor suppressor protein p53 by upregulating Sema3E expression [50].

TGF-β-BMP signaling is involved in developmental morphogenesis and cancer morphogenesis. Morphogens such as those of the TGF-β family inhibit and stimulate basic cell proliferation, respectively, at high and low concentrations. A signaling gradient of declining TGF-β concentration regulates the inhibition and stimulation of cell proliferation [51]. ROS can activate TGF-β either directly or indirectly via the activation of proteases. In addition, TGF-β itself induces ROS production as part of its signal-transduction pathway. Pulmonary tissues are vulnerable to the toxic effects of inhaled air. The oxidant pathways are especially relevant in the lung, where TGF-β is known to have a role in tissue repair and connective tissue turnover. In pulmonary fibrosis and renal endothelial cells, TGF-β activation is considered a hallmark of disease progression [52, 53]. In ovarian cancer, overexpression of FOXG1 contributes to TGF-β resistance through inhibition of p21WAF1/CIP1 expression, which is repressed by p53 [54]. Recent studies have revealed some additional novel functions of the p53 pathway. These include the downregulation of two central cell-growth pathways, the IGF/AKT-1 and mTOR pathways, and the upregulation of the activities of the endosomal compartment [55–57]. The mTOR pathway including the IGF-1/AKT pathway plays critical roles in regulation of cell proliferation, survival, and energy metabolism to shut down cell growth and division to avoid the introduction of infidelity into the process of cell growth and division [58, 59]. In response to stress, IGF-BP3, PTEN, TSC2, AMPK beta1, and Sestrin1/2 are transcribed by p53, play a critical

TABLE 13.2 Oxidative stress-mediated signaling pathways and their related genes

Categorical Pathways Canonical Pathway (ontology)	Gene Name (Symbol)
Reactive Oxygen Species (ROS) Metabolism and Antioxidant Defenses	
Glutathione Peroxidases (GPx)	GPX1, GPX2, GPX3, GPX4, GPX5, GPX6, GPX7, GSTZ1
Peroxiredoxins (TPx)	PRDX1, PRDX2, PRDX3, PRDX4, PRDX5, PRDX6
Other Peroxidases	CAT, CSDE1, CYGB, DUOX1, DUOX2, EPX, GPR156, LPO, MGST3, MPO, PIP3-E, PTGS1, PTGS2, PXDN, PXDNL, TPO, TTN
Other Antioxidants	ALB, APOE, GSR, MT3, SELS, SRXN1, TXNDC2, TXNRD1, TXNRD2
Superoxide Dismutases (SOD)	SOD1, SOD2, SOD3
Other Genes Involved in Superoxide Metabolism	ALOX12, CCS, CYBA, DUOX1, DUOX2, GTF2I, MT3, NCF1, NCF2, NOS2A, NOX5, PREX1, PRG3
Genes Involved in ROS Metabolism	AOX1, BNIP3, EPHX2, MPV17, SFTPD
Oxidative Stress-Responsive Genes	ANGPTL7, ATOX1, CAT, CCL5, CSDE1, DGKK, DHCR24, DUSP1, EPX, FOXM1, GLRX2, GPR156, GSS, KRT1, LPO, MBL2, MPO, MSRA, MTL5, NME5, NUDT1, OXR1, OXSR1, PDLIM1, PIP3-E, PNKP, PRDX2, PRDX5, PRDX6, PRNP, RNF7, SCARA3, SELS, SEPP1, SGK2, SIRT2, SRXN1, STK25, TPO, TTN
p53 Signaling Pathway	
Induction of Apoptosis	BAX, BID, CDKN1A, CRADD, EI24, FADD, FASLG (TNFSF6), FOXO3, PCBP4, PRKCA, TNFRSF10B, TP53, TP73, TP73L
Antiapoptosis	BCL2, BCL2A1, BIRC5, CASP2, HDAC1, IGF1R, MCL1, NFKB1, RELA, TNF, TNFRSF10
Other Apoptosis Genes	APAF1, BRCA1, CASP9, E2F1, GADD45A, GML, LRDD, P53AIP1, SIAH1, SIRT1, TP53BP2, TRAF2
Cell Cycle Arrest	CDKN1A, CDKN2A, CHEK1, CHEK2, GADD45A, GML, MYC, PCAF, PCBP4, RPRM, SESN1, SESN2
Cell Cycle Checkpoint	ATR, BRCA1, CCNE2, CCNG2, CDKN2A, RB1, TP53
Negative Regulation of the Cell Cycle	BAX, BRCA1, CDKN2A, MSH2, NF1, PTEN, RB1, TP53, TP73, TP73L, TSC1, WT1
Regulation of the Cell Cycle	BRCA2, CDC2, CDC25A, CDK4, E2F1, E2F3, HK2, IGF1R, KRAS, PPM1D, PRKCA, STAT1, TADA3L, TP53BP2
Other Cell Cycle Genes	BIRC5, CCNH, CCNB2, ESR1, MLH1, PCNA, PRC1
Negative Regulation of Cell Proliferation	BAI1, BCL2, BTG2, CDKN1A, CDKN2A, CHEK1, GML, IFNB1, IL6, MDM2, MDM4, NF1, PCAF, PPM1D, SESN1
Positive Regulation of Cell Proliferation	IGF1R, IL6
Cell Proliferation	BRCA1, CDC25A, CDC25C, CDK4, E2F1, MYC, PCNA, PRKCA
Cell Growth and Differentiation	ESR1, MCL1, MYOD1
Other Genes Related to Cell Growth, Proliferation, and Differentiation	EGR1, FOXO3A, JUN, KRAS, PTTG1
DNA Repair Genes	ATM, ATR, BRCA1, BTG2, CCNH, DNMT1, GADD45A, MSH2, PCNA, PTTG1, TP53, XRCC5
Human Nitric Oxide Signaling Pathway	
Genes with Nitric Oxide Synthase or Oxidoreductase activity	NOS1, NOS2A, NOS3, NQO1
Positive Regulators of Nitric Oxide Biosynthesis	HSP90AB1 (HSPCB), INS
Negative Regulators of Nitric Oxide Biosynthesis	DNCL1, GLA, IL10

Other Genes Involved in NO Biosynthesis	AKT1, ARG2, DDAH2, DNCL1, EGFR, GCH1, GCHFR
Genes Induced by NO	CDKN1A, IL8, JUN, VEGFA
Genes Suppressed by NO	CCNA1, MYB, TROAP
Genes Involved in NO Signaling Pathway	CAMK1, DLG4, GRIN2D, NOS1, PPP3CA, PRKAR1B, PRKCA
Genes Involved in Superoxide Release	ALOX12, DUOX1, DUOX2, NOX5, PRG3
Genes with Oxidoreductase Activity	ALOX12, CYBA, DUOX1, DUOX2, NOS2A, NOX5, SOD1, SOD2, SOD3
Genes with Peroxidase Activity	DUOX1, DUOX2
Genes with Superoxide Dismutase Activity	SOD2
Other Genes Involved in Superoxide Metabolism	CCS, NCF1, NCF2, PREX1
Antiapoptosis Genes	MPO, MTL5, NME5, PRDX2, RNF7
Genes with Antioxidant Activity	APOE, MT3, SELS, SOD1, SOD3, SRXN1 (C20orf139)
Genes with Glutathione Peroxidase Activity	GPX1, GPX2, GPX3, GPX4, GPX5, GPX6, LOC493869
Genes with Oxidoreductase Activity	CAT, EPX, GPX1, GPX2, GPX3, GPX4, GPX5, GPX6, LPO, MPO, MSRA, PRDX2, PRDX6, SOD1, SOD2, SRXN1(C20orf139), TPO, TXNRD2
Genes with Peroxidase Activity	CYGB, EPX, GPR156, LPO, MPO, PRDX2, PRDX5, PRDX6, TPO, TTN, UNR
Transcription Regulators	FOXM1, GLRX2, SCRT2, SIRT2, SOD2, UNR
Other Genes Involved in Oxidative Stress	ATOX1, DUSP1, GSS, KRT1, MBL2, NUDT1, OXR1, PNKP, PRNP, SCARA3, SEPP1, SGK2
DNA Damage Signaling	
Apoptosis	ABL1, BRCA1, CIDEA, GADD45A, GADD45G, GML, IHPK3, PCBP4, AIFM1 (PDCD8), PPP1R15A, RAD21, TP53, TP73
Cell Cycle Arrest	CHEK1, CHEK2, DDIT3 (CHOP), GADD45A, GML, GTSE1, HUS1, MAP2K6, MAPK12, PCBP4, PPP1R15A, RAD17, RAD9A, SESN1, ZAK
Cell Cycle Checkpoint	ATR, BRCA1, FANCG, NBN (NBS1), RAD1, RBBP8, SMC1A (SMC1L1), TP53
Damaged DNA Binding	ANKRD17, BRCA1, DDB1, DMC1, ERCC1, FANCG, FEN1, MPG, MSH2, MSH3, N4BP2, NBN (NBS1), OGG1, PMS2L3 (PMS2L9), PNKP, RAD1, RAD18, RAD51, RAD51L1, REV1 (REV1L), SEMA4A, XPA, XPC, XRCC1, XRCC2, XRCC3
Base-Excision Repair	APEX1, MBD4, MPG, MUTYH, NTHL1, OGG1, UNG
Double-Strand Break Repair	CIB1, FEN1, XRCC6 (G22P1), XRCC6BP1 (KUB3), MRE11A, NBN (NBS1), PRKDC, RAD21, RAD50
Mismatch Repair	ABL1, ANKRD17, EXO1, MLH1, MLH3, MSH2, MSH3, MUTYH, N4BP2, PMS1, PMS2, PMS2L3 (PMS2L9), TP73, TREX1
Other Genes Related to DNA Repair	APEX2, ATM, ATRX, BTG2, CCNH, CDK7, CRY1, ERCC2 (XPD), GTF2H1, GTF2H2, IGHMBP2, LIG1, MNAT1, PCNA, RPA1, SUMO1
Mitochondria	
Membrane Polarization & Potential	BAK1, BCL2, BCL2L1, BNIP3, SOD1, TP53, UCP1, UCP2, UCP3
Mitochondrial Transport	AIP, BAK1, BCL2, BCL2L1, BNIP3, CPT1B, CPT2, DNAJC19, FXC1 (TIMM10B), GRPEL1, HSP90AA1, HSPD1, IMMP2L, MFN2, MIPEP, MTX2, STARD3, TP53, TSPO, UCP1, UCP2, UCP3
Small Molecule Transport	SLC25A1, SLC25A10, SLC25A12, SLC25A13, SLC25A14, SLC25A15, SLC25A16, SLC25A17, SLC25A19, SLC25A2, SLC25A20, SLC25A21, SLC25A22, SLC25A23, SLC25A24, SLC25A25, SLC25A27, SLC25A3, SLC25A30, SLC25A31, SLC25A37, SLC25A4, SLC25A5
Targeting Proteins to Mitochondria	AIP, DNAJC19, FXC1 (TIMM10B), GRPEL1, HSPD1, IMMP2L, MFN2, MIPEP, TSPO
Mitochondrial Protein Import	AIP, COX10, COX18, DNAJC19, FXC1 (TIMM10B), GRPEL1, HSPD1, MIPEP, SH3GLB1

(*Continued*)

TABLE 13.2 Continued

Categorical Pathways Canonical Pathway (ontology)	Gene Name (Symbol)
Outer Membrane Translocation	TOMM20, TOMM22, TOMM34, TOMM40, TOMM40L, TOMM70A
Inner Membrane Translocation	FXC1 (TIMM10B), IMMP1L, IMMP2L, OPA1, TAZ, TIMM10, TIMM17A, TIMM17B, TIMM22, TIMM23, TIMM44, TIMM50, TIMM8A, TIMM8B, TIMM9
Mitochondrial Fission & Fusion	COX10, COX18, FIS1, MFN1, MFN2, OPA1
Mitochondrial Localization	DNM1L, LRPPRC, MFN2, MSTO1, NEFL, OPA1, RHOT1, RHOT2, UXT
Apoptotic Genes	AIFM2, BAK1, BBC3, BCL2, BCL2L1, BID, BNIP3, CDKN2A, DNM1L, PMAIP1, SFN, SH3GLB1, SOD2, TP53
Hypoxia Signaling	
Response to Hypoxia	ANGPTL4, ARNT2, CREBBP, EP300, HIF1A, MT3, PRKAA1
Response to Oxidative Stress	CAT, CYGB, GPX1, PIP3-E
Immune Response	GPI, IL1A, IL6, IL6ST, NOS2A, NOTCH1, PTX3, RARA
Other Genes Related to Stress Response	ADM, EPO, HYOU1, VEGFA
Hemoglobin Complex-Associated Genes	CYGB, EPO, HBB, HMOX1, NOS2A, PIP3-E
Peroxidase	CAT, CYGB, GPX1, PIP3-E
Other Oxidoreductase-Related Genes	HIF1AN, HMOX1, MT3, NOS2A, PLOD3, TH
Transcription Cofactors	CREBBP, DR1, ENO1, EP300, EPAS1, HTATIP, RARA
Transcription Factors	ARNT2, BHLHB2, CREBBP, ENO1, EP300, EPAS1, HIF1A, HIF3A, KHSRP, MYBL2, PPARA, RARA
Other Transcription Factors and Regulators	HIF1AN, NOTCH1
Antiapoptosis	BAX, ANGPTL4, BIRC5, IL1A, MYBL2, PEA15, PRKAA1, VEGFA
Caspase Activity	BIRC5, CASP1
Induction of Apoptosis	BAX, DAPK3, NUDT2
Other Apoptosis Genes	EP300
Signal Transduction	ADM, ARNT2, CASP1, CDC42, CREBBP, EP300, EPAS1, EPO, GNA11, HIF1A, HIF3A, HMOX1, IGFBP1, IL1A, IL6, IL6ST, IQGAP1, KIT, LEP, PLAU, RARA, VEGFA
Protein Biosynthesis	EEF1A1, PDIA2 (PDIP), PRKAA1, RPL28, RPL32, RPS2, RPS7
Protein Heterodimerization	ARNT2, HIF1A, RARA, SAE1
Protein Homodimerization	ARNT2, RARA, VEGFA
Protein Amino Acid Phosphorylation	DAPK3, KIT, PRKAA1
Protein Binding	CASP1, CREBBP, ENO1, EP300, IQGAP1, NOS2A, PEA15, PPP2CB, RARA
Other Genes Related to Protein Metabolism	ARD1A, CDC42, GNA11, HYOU1, MAN2B1, PLOD3, PSMB3, SUMO2, TUBA4A (TUBA1)
Protease Inhibitors	BIRC5, CSTB
Protease Molecules	AGTPBP1, CASP1, ECE1, PLAU, PSMB3
Other Extracellular Molecules	ADM, ANGPTL4, CHGA, COL1A1, EPO, IGF2, IGFBP1, IL1A, IL6, LEP, NPY, PTX3, VEGFA
Cytoskeleton	DCTN2, SPTBN1
Cell Cycle	BAX, BIRC5, EP300, HK2, IGF2, IL1A, MYBL2, SSSCA1, VEGFA
Cell Proliferation	DCTN2, IGF2, IL1A, IL6, MT3, NPY, RARA, VEGFA
Growth Factors	GPI, IGF2, IGFBP1, IL1A, IL6, KIT, VEGFA
Other Genes Related to Cell Growth	ENO1

Carbohydrate Metabolism	GPI, HK2, LCT, MAN2B1, PEA15, PRKAA1, SLC2A1, SLC2A4
Lipid Metabolism	AGPAT2, ANGPTL4, PPARA, PRKAA1
One-Carbon Compound Metabolism	CA1
Superoxide Metabolism	MT3, NOS2A
RNA Metabolism	PRPF40A (FNBP3), KHSRP, RARA, RPL28, RPS2, SNRP70
Other Genes Related to Metabolism	ADM, AGPAT2, MOCS3, NUDT2, TH, TST, UCP2
Cardiac Excitation-Contraction (E-C) Coupling	ARNT2, CHGA, DAPK3, GNA11, IQGAP1, KIT, NOS2A, NOTCH1, NPY, PRKAA1, SPTBN1
TGF-β BMP Signaling	
TGF-β	TGFB1, TGFB2, TGFB3
BMP	BMP1, BMP2, BMP3, BMP4, BMP5, BMP6, BMP7
GDF	AMH, GDF2 (BMP9), GDF3 (Vgr-2), GDF5 (CDMP-1), GDF6, GDF7, IGF1, IGFBP3, IL6, INHA (inhibin a), INHBA (inhibin BA), LEFTY1, LTBP1, LTBP2, LTBP4, NODAL, PDGFB
Activin	INHA (inhibin a), INHBA (inhibin BA), INHBB (inhibin BB), LEFTY1, NODAL
Receptors	ACVR1 (ALK2), ACVR2A, ACVRL1 (ALK1), AMHR2, BMPR1A (ALK3), BMPR1B (ALK6), BMPR2, ITGB5 (integrin B5), ITGB7 (integrin B7), LTBP1, NR0B1, STAT1, TGFB1I1, TGFBR1, (ALK5) TGFBR2, TGFBR3, TGFBRAP1
SMAD	SMAD1 (MADH1), SMAD2 (MADH2), SMAD3 (MADH3), SMAD4 (MADH4), SMAD5 (MADH5)
TGF-β/Activin-Responsive	CDC25A, CDKN1A (p21WAF1 / p21CIP1), CDKN2B (p15LNK2B), COL1A1, COL1A2, COL3A1, FOS, GSC (goosecoid), IGF1, IGFBP3, IL6, ITGB5 (integrin B5), ITGB7 (integrin B7), JUN, JUNB, MYC, PDGFB, SERPINE 1 (PAI-1), TGFB1I1, TSC22D1 (TGFB1I4), TGFBI, TGIF1
BMP-Responsive	BGLAP (osteocalcin), DLX2, ID1, ID2, JUNB, SOX4, STAT1
Molecules Regulating Signaling of the TGF-β Superfamily	BAMBI, BMPER, CDKN2B (p15LNK2B), CER1 (cerberus), CHRD (chordin), CST3, ENG (Evi-1), EVI1, FKBP1B, FST (follistatin), HIPK2, NBL1 (DAN), NOG, PLAU (uPA), RUNX1 (AML1), SMURF1
Adhesion Molecules	BGLAP (osteocalcin), ENG (Evi-1), ITGB5 (integrin B5), ITGB7 (integrin B7), TGFB1I1, TGFBI
Extracellular Matrix Structural Constituents	BGLAP (osteocalcin), COL1A1, COL1A2, COL3A1, LTBP1, LTBP2, LTBP4, TGFBI
Other Extracellular Molecules	AMH, BMP1, BMP2, FST (follistatin), GDF2 (BMP9), GDF3 (Vgr-2), IGF1, IGFBP3, IL6, INHA (inhibin a), INHBA (inhibin BA), INHBB (inhibin BB), PDGFB, PLAU (uPA), SERPINE1
Transcription Factors and Regulators	DLX2, EVI1, FOS, GSC (goosecoid), HIPK2, ID1, JUN, JUNB, MYC, NR0B1, RUNX1 (AML1), SMAD1 (MADH1), SMAD2 (MADH2), SMAD3 (MADH3), SMAD4 (MADH4), SMAD5 (MADH5), SOX4, STAT1, TGFB1I1, TSC22D1 (TGFB1I4), TGIF1
Tumor Necrosis Factor (TNF) Ligand and Receptor	
Induction of Apoptosis	CASP2, CASP3, CASP8, CRADD, FADD, FAS, FASLG, LTA, TNFSF8, TNFRSF10, TNFRSF10A, TNFRSF10B, TNFSF14, TNFRSF19, TNFRSF25, CD27 (TNFRSF7), TNFRSF9, TRADD
Caspase Activation	TNFRSF10A, TNFRSF10B, TNFSF15
Caspase Inhibition	CD27 (TNFRSF7), TNFSF14
Anti-apoptosis Genes	CD40LG, FAS, TNF, TNFRSF10D, TNFRSF6B, CD27 (TNFRSF7), TNFSF18
Other Apoptosis-Related Genes	CD40, CD70 (TNFSF7), TNFSF9, LTBR, NGFR, TNFRSF10C, TNFRSF11B, TNFRSF12A, TNFRSF14, TNFRSF1A, TNFRSF1B, TNFRSF21, DFFA, PAK1, TRAF2
Inflammatory Response	CD40LG, TNF, TNFRSF1A
NF-κB Signaling Pathway	CASP8, FADD, TNF, TNFRSF1A, FASLG, TNF, TNFSF10, TNFSF14, TNFSF15, CD40, EDA2R, LTBR, TNFRSF10A, TNFRSF10B, CD27 (TNFRSF7), TRADD

(*Continued*)

TABLE 13.2 Continued

Categorical Pathways Canonical Pathway (ontology)	Gene Name (Symbol)
JNK Signaling Pathway	EDA2R, TNFRSF19, CD27 (TNFRSF7), MAP2K4, MAPK8, PAK1
Other TNF Superfamily Members and ligands	LTB, PGLYRP1, TNFSF11, TNFSF12, TNFSF13, TNFSF13B, TNFSF4, TNFSF5IP1, TNFRSF11A, TNFRSF13B, TNFRSF13C, TNFRSF17, TNFRSF19L, TNFRSF4, TNFRSF8
Transcription Regulators	JUN, PARP1, RB1, TNF, TNFRSF1A, TNFRSF25, CD27 (TNFRSF7), TNFRSF9
TNFR1 Signaling Pathway	
FAS signaling pathway	ARHGDIB, CAD, HRB, LMNA, LMNB1, LMNB2, MADD, MAP3K1, MAP3K7, PAK2, PRKDC, SPTAN1
Induction of Apoptosis	IKBKG, LTA, TRAF3, TNFRSF14, TNFRSF1A, TNFRSF1B
Anti-apoptosis Genes	NFKB1, TNFAIP3
Other Apoptosis Genes	NFKBIA, TNFRSF1B, TRAF1, TRAF2
Inflammatory Response	NFKB1
NF-κB Signaling Pathway	CHUK, IKBKB, IKBKG, NFKBIA, TNFAIP3
Transcription Regulators	IKBKB, IKBKG, NFKB1, NFKBIA
TNFR2 Signaling Pathway	DUSP1, HRB, IKBKAP, MAP3K1, MAP3K14, TANK

role as negative regulators, and lead to the reduction in the activities of these two pathways. Furthermore, p53 transcriptionally regulates TSAP6, Chmp4C, Caveolin-1, and DRAM, which are critical genes in the endosomal compartment, increases exosome secretion and the rate of endosomal removal of growth factor receptors from cell surface, and enhances autophagy [60–63]. It is thought that these p53-mediated activities slow down cell growth and division, conserve and recycle cellular resources, communicate with adjacent cells and dendritic cells of the immune system, and inform other tissues of the stress signals [55, 64, 65].

TNF ligand-receptor signaling occurs because TNF, as a multifunctional cytokine, can induce cell death through receptor-mediated caspase activation and mitochondrial dysfunction by a trigger of oxidative stress induced in cardiovascular disease, neuronal disease, and cancer [66]. Opposing these cell death-promoting signals, binding of TNF receptors can also trigger survival signal activation. A critical balance among various intracellular signaling pathways determines the predominant in vivo bioactivity of TNF, as best exemplified by the differential responses of various organs.

A major source of ROS in cells is the mitochondria. Electron leakage from the mitochondrial respiratory chain can react with molecular oxygen, resulting in the formation of the superoxide anion radical, which can subsequently be converted to other ROS. In phagocytes and some cancer cells, ROS can be produced through a reaction that is catalyzed by NADPH oxidase complexes. When attackers from the outside, such as environmental stressors, damage mitochondria, electron leakage is also induced; this dysfunction induces severe problems in tissues [67–70]. Mitochondrial dysfunction causes the onset of some diseases [71–74]. Recent evidence has shown that mitochondrial dysfunction is related closely to insulin resistance and metabolic syndrome. The underlying mechanism of mitochondrial dysfunction is very complex, including genetic factors from both the nucleus and mitochondrial genome, with numerous environmental factors also impacting [75].

Exposure to air pollution, including particles, metals, and other organic compounds as environmental stressors, is associated with pulmonary diseases and cancer. The mechanisms of induced health effects are believed to involve oxidative stress. Oxidative stress mediated by airborne particles and/or fibers might arise from direct generation of ROS from the surfaces of particles and fibers, soluble compounds such as transition metals or organic compounds, and activation of inflammatory cells capable of generating ROS and RNS. Generation of ROS/RNS can cause covalent modifications to DNA directly, or they can initiate the formation of genotoxic lipid hydroperoxides. The resulting oxidative DNA damage can engender changed gene expression such as upregulation of tumor promoters and downregulation of tumor suppressor genes; the DNA damage might therefore be implicated in cancer development. This chapter describes the important role of free radicals in particle- and fiber-induced cellular damage, the interaction of ROS with target molecules, especially with DNA, and the modulation of specific genes and transcription factor caused by oxidative stress. Consequently, various environmental stressors cause cellular damage through oxidative stress induction and many signaling pathways. However, what environmental stressor is dominant in which signaling pathway is not always clear. Therefore, identifying gene expression signatures extracted from microarray data can clarify how environmental stressors may damage cells and engender diseases.

13.2.1 Case Studies in Tissues or Organs from Rats Exposed to Environmental Stressors

Many animal models have been studies to elucidate mechanisms of action of oxidants or antioxidants. Research on oxidative stress and its defense has expanded dramatically because of its potential benefit in disease prevention and health promotion. In particular, rats exposed to stress-induced chemicals have been extensively studied in biological systems such as cell cultures, animal models, and clinical trials [76–79]. Therefore, 33 independent studies in rats are focused on in this chapter because these studies used microarrays for which gene expression data are publicly available from the Gene Expression Omnibus (GEO; http://www.ncbi.nlm.nih.gov/gds). Those microarray data with the same platform GPL341 (Affymetrix) sets in rats were downloaded for this study. All data sets were normalized across all arrays by Z-score transformation methods after combination with respect to probe IDs. The normalized values were filtered with oxidative-related genes listed in this work (Table 13.2), and then the top 10 genes from the upregulated and downregulated genes were chosen to analyze gene expression signatures (Table 13.3). The selected genes were classified by using principal component analysis to create gene expression signatures of oxidative stress and were divided into six groups. Most selected genes could be assigned to gene ontology (GO) categories: DNA repair, oxygen and reactive oxygen species metabolism, and response to stress, but cyclins and cyclin dependent kinase contained in "Apoptosis related genes, Cell Cycle Arrest and Checkpoint, Regulation of the Cell Cycle, Regulation of Cell Proliferation, Cell Growth and Differentiation" of "p53 signaling" and "TGF-beta signaling" were not observed. Experimental conditions selected from GPL341 data sets in this work were almost all of short-period exposure using in vivo and in vitro culture systems of rats. It is noteworthy that

TABLE 13.3 Environmental stressors induce different gene expression signatures

Environmental Stressors (target organ or tissues)	Up-gene	Down-gene	GEO ID
Cluster 1			
Methylprednisolone (kidney)	Apoe, Gpx2, Ngb, Nos2, Prdx6, Tmod1, Tnp1, Tpo	Brca2, Cry2, Fen1, Hus1, Ptgs2, Pttg1, Rad50, Srxn1, Xrcc6	GDS964
Methylprednisolone (liver)	Aass, Atrx, Ncf1, Nqo1, Scd1, Slc41a3, Srd5a2, Tmod1, Tnp1	Chek1, Cry2, Lig1, Mgmt, Pold1, Pold3, Rad50, Rad52, Smc3, Xrcc6	GDS972
Streptozotocin (penile cavernosal)	Apc, Cat, Duox2, Gpx2, Gpx6, Gsr, Lpo, Slc38a1, Smc3, Tpo	Atrx, Gpx7, Nos2, Park7, Ptgs2, Scd1, Slc38a4, Slc41a3, Srxn1, Zmynd17	GDS1393
Trimethyltin (hippocampus)	Apex1, Dnm2, Fancc, Gpx7, Lpo, Mgmt, Park7, Prnp, Txnip, Ucp3	Apc, Apoe, Hbz, Mpp4, Ptgs2, Smc3, Srd5a2, Tnp1, Tpo	GDS2555
Octreotide (gastric ECL)	Brca1, Brca2, Dnm2, Duox2, Msh2, Nox4, Tmod1, Tpo, Xirp1	Apex1, Atrx, Cry2, Gpx6, Nos2, Slc38a1, Slc38a4, Slk, Tmod1, Tpo	GDS2558
Cluster 2			
Fibronectin (ventricular myocytes)	Apoe, Atrx, Chaf1a, Ngb, Rad51c, Smc3, Srxn1, Tpo, Zmynd17	Actb, Atrx, Gsr, Mutyh, Ngb, Prdx6, Rad52, Smc3, Tpo, Txnrd1	GDS696
Protein restriction (visceral adipose tissue)	Aass, Apc, Gpx6, Gstk1, Ngb, Prnp, Rad51c, Scd1, Tmod1, Tnp1	Brca2, Chaf1a, Lpo, Mutyh, Nos2, Pttg1, Slc38a1, Slc38a4, Tpo, Ung	GDS880
Heregulin (ureteric buds)	Dhcr24, Hus1, Ldha, Mif, Park7, Rad1, Rad50, Scd1, Tdg, Ung	Actb, Atrx, Nos2, Nox4, Nqo1, Ptgs1, Rad23a, Srxn1, Txnrd1	GDS1518
Kainic acid (hippocampi)	Apoe, Brca2, Ncf1, Nox4, Pold1, Rad23a, Rad50, Rad51c, Srd5a2, Tmod1	Chaf1a, Hbz, Lpo, Mb, Pold3, Tnp1, Tpo, Ucp3, Ung, Zmynd17	GDS1626
Ethanol (pancreas)	Apoe, Atrx, Hbz, Ogg1, Ptgs2, Scd1, Srxn1, Tmod1, Txnrd2, Zmynd17	Cry2, Hus1, Mb, Msh2, Nox4, Nthl1, Prdx6, Rad52, Slk, Srd5a2	GDS2107
Sulfur dioxide (lung)	Aass, Brca1, Cry2, Hus1, Nos2, Ptgs2, Pttg1, Rad50, Tpo, Zmynd17	Apex1, Brca2, Gpx6, Nos2, Nox4, Rad23a, Rad51c, Srd5a2, Tnp1, Tpo	GDS2372
Hypoxia (adrenal gland)	Chaf1a, Duox2, Ldha, Ngb, Pold3, Rad23a, Slc41a3, Tpo, Txnrd2	Aass, Apc, Apoe, Atrx, Cry2, Lpo, Nox4, Rad52, Srd5a2, Tnp1	GDS2457
Methylprednisolone (skeletal muscles)	Aass, Atrx, Hbz, Ngb, Rad1, Scd1, Slc38a5, Tmod1, Tpo, Xirp1	Als2, Atrx, Brca2, Cat, Gsr, Ncf1, Nox4, Nqo1, Slc41a3, Trpc2	GDS2688
Cluster 3			
Forskolin (pheochromocytoma cell)	Aass, Apex1, Brca1, Chek1, Duox2, Gpx2, Hbz, Nxn, Ptgs1, Pttg1	Atrx, Cat, Cygb, Ehd2, Gpx3, Gpx4, Gpx7, Scd1, Sod3, Vim	GDS1363
N-methyl-*N*-nitrosourea (mammary tumors)	Cat, Ehd2, Gadd45a, Gstk1, Mgmt, Prdx3, Prdx6, Scd1, Srxn1, Ube2a	Dpagt1, Gab1, Gpx3, Lpo, Mpg, Nxn, Prdx4, Prnp, Rad52, Txnip	GDS1452
Retinoic X receptor ligand LG100268 (mammary gland)	Brca1, Dnm2, Gpx6, Hbz, Mpp4, Ncf1, Nos2, Slc38a1, Tpo	Aass, Atrx, Chaf1a, Gsr, Idh1, Nox4, Prdx1, Rad23a, Xrcc1, Zmynd17	GDS1922
Angiopoietin-1 (aortic rings)	Apex1, Dnm2, Mgmt, Ngb, Pold3, Rad50, Slc38a1, Srd5a2, Srxn1, Ucp3	Atrx, Brca2, Chaf1a, Gpx6, Mb, Nox4, Rad23a, Slk, Tpo, Zmynd17	GDS2037